Development and Application of an Online Transient Coupled Groundwater-Surface Water Model in Indus Basin

M.Sc. Thesis by Haochen Yuan

April 2024

Water System and Global Change Group

Development and Application of an Online Transient Coupled Groundwater-Surface Water Model in Indus Basin

M.Sc. Thesis by Haochen Yuan

Author:	Haochen Yuan
Student Number:	1251880
Study Program:	Environmental Sciences
Chair Group:	Water System and Global Change
Supervisor 1:	dr.ir. IEM (Inge) de Graaf
Supervisor 2:	Sida Liu

Wageningen University & Research, Wageningen, the Netherlands

April 9, 2024

Acknowledgements

I would like to express my sincere gratitude to all those who have contributed to the completion of this master's thesis. Without these kindly help I couldn’t have the possibility to finish it successfully.

The first and foremost ones come to my mind are my supervisors, Inge de Graaf and Sida Liu. I am deeply thankful to all of them for their invaluable guidance, continuous support, and encouragement throughout this journey. I vividly recall my initial encounter with Inge, during which she generously offered valuable suggestions for my course study and proposed potential thesis topics. Throughout my thesis study, Inge remained reachable and attentive, consistently providing useful suggestions and support. She also taught me to take my time to work and if problems exist, be patient to check it step by step. That really helps.

My direct supervisor, Sida Liu, provided assistance not only in scientific guidance and study methodology but also offered emotional support. Whenever I need help, she was always patient and peace. She could even sit together with me to check the problems one by one. It is because of her presence that I often felt reassured and was willing to spend a considerable amount of time solving a problem. She also gave lots of comments on my report, which really helped me to improve it. I am deeply grateful to her.

I also want to appreciate my family as well as my girlfriend, Qi Su. They are always the ones who I can trust and discuss the pressures with. Despite the time difference and thousands of kilometres apart, they cared about me every day and visited the Netherlands to accompany me at different times, which provided me with a lot of emotional support.

Thanks to all of my friends here. Over the study of a year and a half, they have been the individuals I could easily reach out to in times of joy or distress, and together, we have created many cherished memories.

In all, thank to everyone I met and everything I experienced. It shapes me myself today.

Abstract

Groundwater, as one of the most important freshwater resources in this world, supports billions of people's livelihood and economic growth of various countries. It also plays a vital role in the global water cycle and contribute to the total water storage. However, during the past decades, groundwater is sometimes overlooked in water availability worldwide evaluation processes. The VIC-WUR macroscale hydrological model, which can simulate multiple natural hydrological processes and human impacts on global water resources, still lacks a good representation of the groundwater aquifers, causing an inaccurate estimation of the groundwater availability.

To address this problem, The VIC-WUR hydrological model has been coupled with a MODFLOW6 model and tested by a case study in Indus Basin. It is realized by replacing the bottom layer of the VIC-WUR model with a two-layer groundwater model constructed by MODFLOW6. The VIC-WUR model supplies groundwater recharge and river discharge data to MODFLOW6, while MODFLOW6 updates baseflow and capillary rise information to the VIC-WUR model. With the use of MODFLOW6, the lateral groundwater flow can be simulated. In this study three different coupling schemes have been evaluated: offline coupling (OFC), partially online coupling (POC) and fully online coupling (FOC). OFC settings allow MODFLOW6 to run completely after VIC-WUR. POC and FOC run the two models in each time period consecutively, while the former only consider baseflow but the latter one also takes capillary rise into account.

Under naturalized condition (NatCon), which only reflects the impact of historical climate variations, the three coupling models are tested. The majority of the Indus Basin's groundwater level (GWL) range from 0 to 2000 m, with value exceeding 5000 m in the mountainous areas. Under OFC, among the six selected cells, the monthly GWL difference ranges from 0.02 m to 5.08 m. In the upper and middle basin, GWL decrease, while in the remaining cells, there is a slight increase in GWL, peaking around summer. The total groundwater discharge throughout the analyse period is approximately 70 times greater than river leakage, with different seasonal variation. FOC estimates groundwater discharge higher than OFC by 2.02% on average across twelve months. River leakage decreases under FOC compared to OFC, ranging from 17.49% to 86.76% across twelve months. Compared to POC, FOC predicts slightly lower groundwater discharge by 0.29% on average. Overall, FOC estimates 0.42% less river leakage than POC, mainly in the summer months. Simultaneously, following changes in baseflow, GWL exhibit a delayed response, typically peaking half a month to a month later.

Under human impact condition (HumanCon), which considers not only historical climate but also human activities impact, only the offline coupling model is run (OFC-HumanCon). There is a noticeable decline in GWL in the middle and lower basins. Across six cells, GWL declines are between 0.01 to 8.15 m. In total, 20% areas show GWL drawdown less than 10 meters. Most of the upper basin experience drawdown

within 1 m. Over 80% of the agriculture region show drawdown over 20 m. In lower basin, most areas near rivers have GWL declines ranging from 1 to 10 m. The upper, middle and lower basin frames show GWD at an average of 0.67, 56, 9.67 km^3/yr, which are larger than other studies.

The coupling schemes are compared with the original VIC-WUR model. The maximum discharge in the original VIC-WUR model is 12105.40 m^3/s while the number in FOC model is 11951.70 m^3/s. In the upstream, FOC model simulates river discharge 7.00% lower than the original VIC-WUR model. However, in the midstream and downstream, the coupling model predicts higher river discharge than the original VIC-WUR model, with increases of 4.97% and 0.23%, respectively. During low-flow periods, the FOC model predicts river flow values up to 2.53 times higher than those of the original VIC-WUR model. Conversely, during high-flow periods, the FOC model forecasts up to a 26.90% lower discharge compared to the original VIC-WUR model.

In all, the three coupling schemes are plausible and well-performed in Indus Basin. They all present distinct strengths in calculating components in hydrological models. It could improve the understanding and estimation of surface and groundwater availability.

Keywords: Groundwater modelling; Indus Basin; coupling models; VIC-WUR; MODFLOW6

Table of Contents

List of figures and tables

List of abbreviations

OFC	Offline Coupling
POC	Partially Online Coupling
FOC	Fully Online Coupling
NatCon	Naturalized Condition
HumanCon	Human Impact Condition
GWD	Groundwater Depletion
GWL	Groundwater Level
TWS	Total Water Storage
GWDE	Groundwater Depth
GWLSS	Steady-State Groundwater Level
GWS	Groundwater Storage
GWSA	Groundwater Storage Anomaly
Ltma	Long-term monthly average

Ch1 Introduction

1.1 Research background

Groundwater, as the largest accessible freshwater resources for humans, serves as a lifeline for billions across the globe, supporting their livelihoods and facilitating the economic growth, a trend that is increasingly pronounced (Yu et al., 2018). Globally, about 25% of anthropogenic water demand relies on groundwater, contributing 50% to drinking water, 40% to industry and 20% to irrigation (Hao et al., 2018). Within the global water cycle, groundwater also plays a fundamental and pivotal role (Condon et al., 2021). It could not only mitigate the excess rainfall from short-time extreme precipitation events by accepting water infiltrated through soil layer, but also act as a vital buffer to discharge water to river to against water scarcity during droughts (Kuang et al., 2024). In this way, groundwater could storages more than 23 million km^3 water in this world, as shown in Figure 1. It is a crucial sector in the management of global water resources, playing a vital role in ensuring water availability and sustainability (Gleeson et al., 2010).

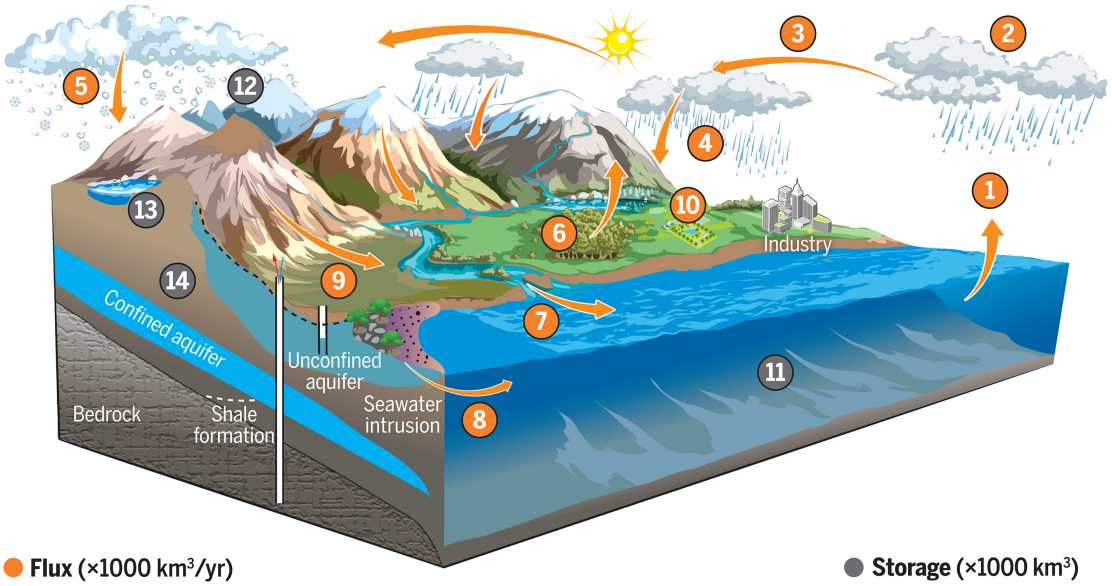

Flux (×1000 km³/yr)
1 Ocean evaporation (420 ± 20%)
2 Precipitation on ocean (380 ± 20%)
3 Net water vapor flux transport (46 ± 20%)
4 Rainfall (98.5 ± 10%)
5 Snowfall (12.5)
6 Terrestrial evapotranspiration (69 ± 10%)
7 Runoff (46 ± 10%)
8 Groundwater discharge (4.5 ± 70%)
9 Groundwater withdrawal (~1.0)
10 Managed aquifer recharge (MAR) 0.01

Storage (×1000 km³)
11 Ocean 1,338,000
12 Glaciers and snow 24,064
13 Permafrost 300
14 Groundwater 23,400

Figure 1 Global water cycle (Kuang et al., 2024)

In recent years, due to the changing climate and rising temperature worldwide, significant hydrological changes are expected to happen and lots of people may suffer from the water resources problems (Khan et al., 2020). Thus, lots of researchers are trying to evaluate the large-scale water availability. Building hydrological models is an efficient way in that as it simulates the water flow system both in spatial and temporal

scale (Khan et al., 2020). These models have the capability to simulate global or regional hydrology and associated processes, yielding insights into meteorological phenomena, water balance dynamics, pollutant transport, surface runoff patterns, energy fluxes, and more. Examples include the WBM-WTM model, ECHAM model, VIC model, PCR-GLOBWB, WaterGAP model, among others (Sood & Smakhtin, 2015). However, groundwater has always been overlooked in the model although it is a non-neglectable component indeed (Condon et al., 2021). Fortunately, in recent years, more and more scientists come to realize the importance of considering groundwater in global water resources research, prompting the incorporation into existing frameworks (de Graaf et al., 2019; Burek et al., 2020; Gerdener et al., 2023). This shift enhances the model complexity and improves the accuracy and reality of the hydrological model representation.

The VIC-WUR model is a macroscale hydrological model, capable of simulating the multiple natural hydrological processes and human impacts on global water resources (Hamman et al., 2018). However, the current version of VIC-WUR regarding groundwater is a simplistic approach (Droppers et al., 2020). It incorporates a groundwater layer that receives infiltration from soil moisture and generates baseflow as a result, which means the groundwater does not flow between cells (Figure 2). It also views groundwater withdrawals as a linear extraction from an unlimited aquifer below the soil column and moreover, does not simulate the groundwater flow exchanges between cells nor between groundwater/surface water and groundwater/soil moisture, which are unrealistic (de Graaf et al 2015). By not simulating the above listed interactions and fluxes, estimates of groundwater availability are substantial lower and consequently, estimates of groundwater depletion (hereafter refers as GWD) are substantially higher, especially in the regions where groundwater pumping rates are high (de Graaf et al., 2019; de Graaf & Stahl, 2022). Moreover, a proper aquifer parameterization is lacking in the current VIC-WUR model, which could improve the representation of the current groundwater layer (Droppers et al., 2020).

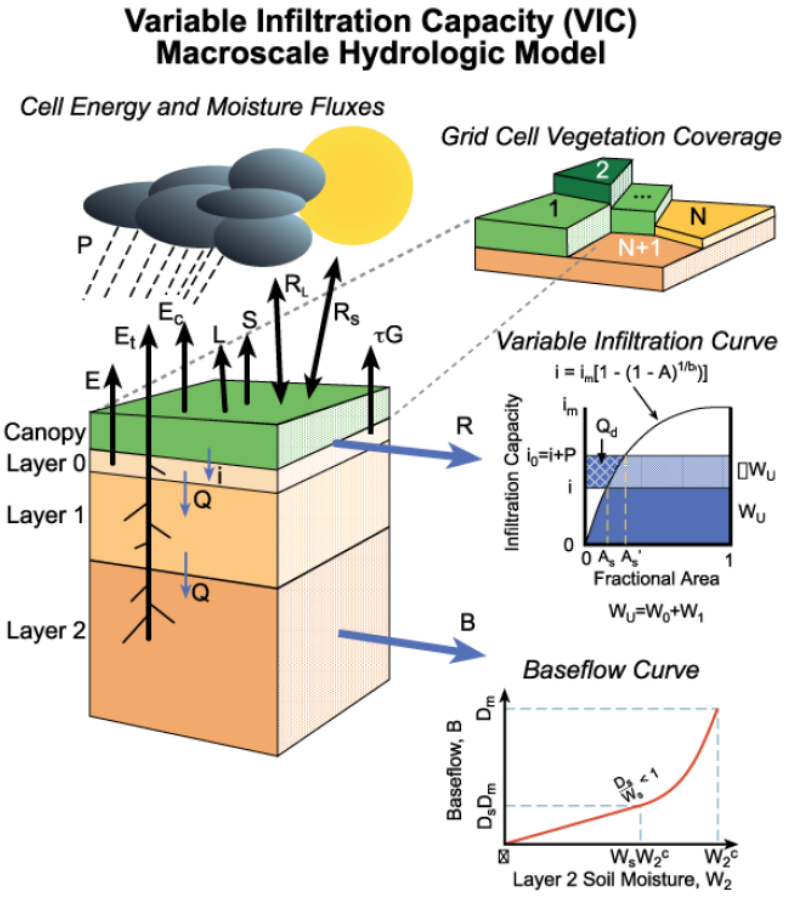

Figure 2 VIC model design (retrieved from VIC-website University of Washington)

Therefore, to obtain more reliable estimates of groundwater availability and its interactions with surface water and soil moisture, the current groundwater representation in VIC-WUR has to be replaced with a real groundwater flow model. In this study, the Indus Basin is selected as the research area to simulate and test as it has a long history of groundwater use and is experiencing crisis in terms of groundwater use (Droppers et al., 2022). Detailed information of the area will be given in the following section.

1.2 Research area

The Indus Basin is located in the southwest of Asia, drained by the Indus River (Laghari et al., 2012). The catchment area is shared by four countries: Pakistan, India, Afghanistan and China, in order from the most to the least (Laghari et al., 2012), as shown in Figure 3. The total basin area spans an area of around 1.13 million km^2 which is composited by various topographical regions (Cheema & Qamar, 2019), as defined by International Water Management Institute. The elevation of the basin ranges approximately from 0 to 6100 meters, with over 40% of it locates above 2000 m above sea level (Cheema & Qamar, 2019). The total basin could be divided into two physiographic divisions: the upper mountain part consisting of Himalaya, Karakoram, Hindu Kush, Shiwalik, Suleiman and Kirthar ranges, with an attitude greater than 5000 m (Cheema & Qamar, 2019); and the mid-lower agriculture intensive alluvial plains,

including the Punjab and Sindh Provinces (Laghari et al., 2012).

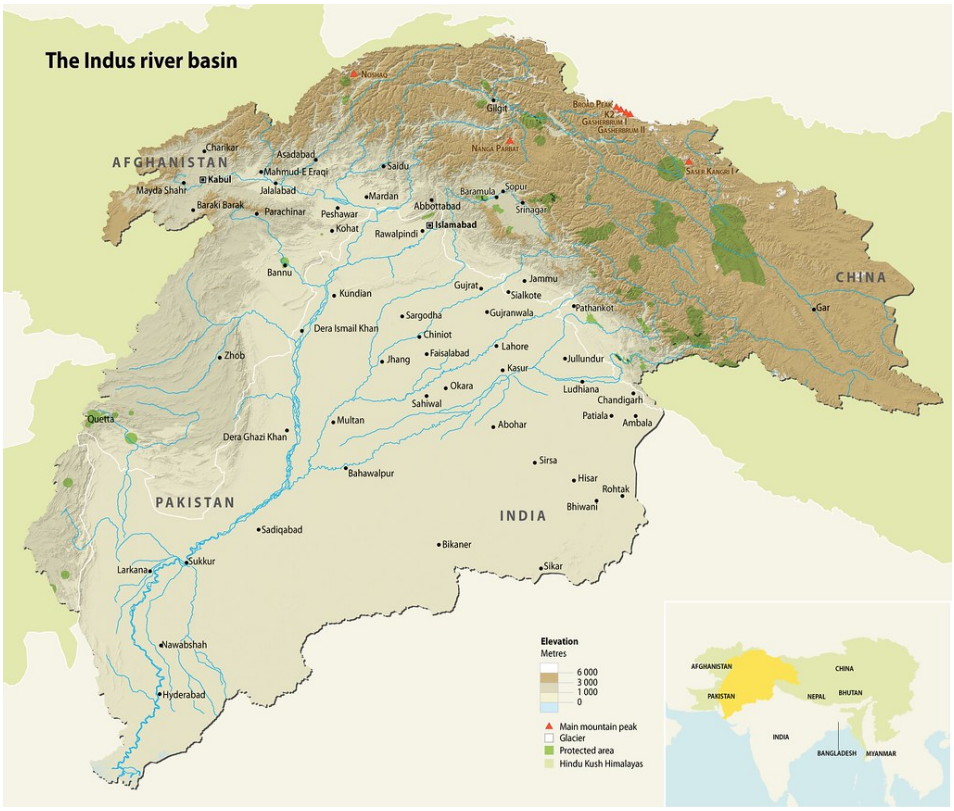

Figure 3 The Indus Basin (https://www.grida.no/resources/6692)

The climate in Indus Basin is complex due to the large area of high mountains. Overall, most of the basin is arid or semi-arid, with the exception in Himalayan mountainous area which receives significant rainfall (A. B. Shrestha et al., 2019). The mean annual precipitation varies between 90 mm and 500 mm in the middle agriculture area and downstream plains, while it could reach more than 1000 mm in the upper catchment (A. B. Shrestha et al., 2019). The average temperature varies a lot, from 2℃ in winter to 49℃ in summer. According to A. Ali (2013), the average annual evaporation ranges between 1650 mm to 2040 mm, leading to the aridity of the basin.

The Indus Basin includes the largest permanent glacial ice outside the polar regions, with an area of 37,134 km^2 (Laghari et al., 2012; A. Shrestha et al., 2015). Since the terrain is high in the northeast and low in the southwest, the river also shows this flow trend from the north to the south, east to the west. Approximately, 80% of the runoff in the upper basin are from meltwater from glaciers in Himalaya, Hindu Kush and Karakorum mountains (A. B. Shrestha et al., 2019). Therefore, the river flow always reaches its peak in summer, which results in substantial floods in this area (A. Ali, 2013).

The mid-lower part in Indus Basin has the largest contiguous irrigation system and is one of the most densely populated and agriculture intensive region in this world (Dahri et al., 2016). It carries the livelihoods of over 240 million people from Pakistan, India, Afghanistan and China (Droppers et al., 2022; Smolenaars et al., 2022). Agriculture supports more than half of the inhabitants in Indus Basin and is one of the most

important development strategies of India and Pakistan (Droppers et al., 2022). Major agriculture zones such as Sindh, Haryana and Punjab province lie along the mid-southern downstream part. In general, in the upper basin, the irrigation water is mostly from the wet mountainous area as the glacial area is very large. While in the downstream area, excessive extractions of groundwater accounts for about 29% to 59% of the irrigation needs (Cheema et al., 2014; Droppers et al., 2022). In Punjab province, this number even rises to 90% (Qureshi et al., 2010), which makes groundwater withdrawal exceeds the recharge (Cheema et al., 2014; Droppers et al., 2022). Moreover, to sustain the stable and sufficient production of croplands, more than 95% of the irrigated water was obtained from blue water withdrawals (Laghari et al., 2012), which leads to the consequence that many of the wells are running dry due to dropping water table depths which are falling at an annual average rate of 2 to 3 m (Qureshi et al., 2010). A large area of the basin is experiencing a severe GWD (de Graaf et al., 2017), combined with salinity problems and flooding, which poses potential threats to local water resources (Laghari et al., 2012; Droppers et al., 2022). It is expected that the population in the region and water demand for food production will increase in the following years, bringing challenges to development of Indus Basin (Vinca et al., 2021). It is essential to have a holistic and detailed vision of the current water storage and availability in Indus Basin, by constructing the hydrological model considering groundwater flow system (Laghari et al., 2012; Arshad et al., 2022).

1.3 Research objectives and questions

The general objective of this research is to simulate the surface water and groundwater availability in Indus basin by different modelling schemes under naturalized and human impact condition (hereafter refers as NatCon and HumanCon respectively). The NatCon aims to reflect the influence of sole historical climate change, while the HumanCon seeks to reflect the consequences of anthropogenic activities encompassing industrial, agricultural, and domestic water use, among others. To achieve this, this study integrated the VIC-WUR model with groundwater flow model by MODFLOW6, in three kinds of coupling schemes: Offline coupling (hereafter refers as OFC), partially online coupling (hereafter refers as POC) and fully online coupling (hereafter refers as FOC), which accounts for the lateral groundwater flow and groundwater storage (hereafter refers as GWS) change. For this study, it is expected to enhance the model performance by having a better representation of the surface water-groundwater interaction and water exchange between the vadose and saturated zone, by building and running the model in Indus Basin.

The general research question is:

What are the differences in the estimations of the groundwater and surface water availability with and without adding groundwater flow model in Indus Basin?

The sub research questions are:

What are the impacts of historical climate variations on groundwater flow system in

Indus basin?

What are the impacts of human activities on groundwater flow system in Indus basin?

How does the groundwater impact the surface hydrological components in Indus Basin?

1.4 Thesis report structure

This report consists of six chapters: Introduction, Literature Review, Methodology, Result Analysis, Discussions, Conclusions and Prospects. In Introduction, the research background, research area and the research objectives are given, providing the fundamental statement of the thesis.

In Literature Review, a brief overview of the current research related to water availability in Indus Basin was provided, followed by model introduction of VIC-WUR model and MODFLOW6 model.

In the subsequent chapter, the research methodology of this thesis was delineated. This chapter elaborated on the coupling approaches of all three coupling schemes. Furthermore, it presented the conceptual model, encompassing boundary conditions, initial conditions, sources and sinks, and all other requisite settings. Subsequently, methods for data acquisition and processing, along with simulation settings for all schemes and conditions, were provided. For both NatCon and HumanCon, the selected input and output settings were outlined.

In the Result Analysis section, the content was divided into three parts: NatCon simulation, HumanCon simulation, and comparison between the two conditions. The main analysed characteristics involved groundwater level (hereafter refers as GWL), baseflow (including river leakage and groundwater discharge), and GWD, in terms of spatial distribution and temporal variation.

Following the Result Analysis, the discussion section presented comparison studies. Here, the importance of baseflow modelling was realized by comparing river discharge with and without feeding baseflow back after MODFLOW6 simulation for each stress period, which involved online coupling and offline coupling. Additionally, by considering capillary rise into the model, the fully online coupling model was compared with the original VIC-WUR model to demonstrate the contribution of groundwater in the hydrological model, considering seasonal and spatial differences.

The Conclusion and Prospect chapter served as the final chapter. It firstly provided the final statements of key findings and achievements in this study. Then, a prospect of the development and application of the coupling hydrological model with the groundwater model was provided to showcase the potential improvement of such model framework in the future.

Ch2 Literature Review

2.1 Current research

The Indus Basin, confronting significant challenges in its water sectors and facing a prolonged water crisis, has been subject to extensive research aimed at quantifying water availability and assessing related impacts. As a consequence of excessive abstraction of groundwater, Northern India and adjacent areas were losing groundwater at a rate of 54 ± 9 km^3/yr between 2002 and 2008 and for the Indus Basin this number is rough 10 km^3/yr, from satellite-based Gravity Recovery and Climate Experiment (GRACE) estimates of total water storage (hereafter refers as TWS) change (Tiwari et al., 2009). However, the observed TWS by GRACE accounts for the total groundwater, surface runoff, soil moisture, and canopy water (S. Ali et al., 2022). Therefore, sometimes it is not applicable to quantify total GWS as TWS is affected by various components (Döll et al., 2014). By analysing the groundwater storage anomaly (hereafter refers as GWSA) in sub river basins in Indus Basin, Akhtar et al. (2022) derived the GWD for the Lower Bari Doab Canal and the Kabul River Basin at values of 4.87 m and 4.82 m during 2002 – 2017. Climate change projections indicate an increase in flash floods, which is expected to further diminish recharge rates and elevate runoff levels (Akhtar et al., 2022). Unfortunately, the coarse resolution of GRACE data impedes the identification of localized hotspots in GWS variations (Arshad et al., 2022). Therefore, Akhtar et al. (2022) downscaled the GRACE data and combined it with Soil and Water Assessment Tool (SWAT). It was calculated that between 2002 and 2019, Dehli Doab experienced the highest loss of over 50 km^3, followed by upstream areas with losses ranging from 7.8 to 49 km^3, and downstream areas with losses ranging from 0.77 to 7.77 km^3 (Akhtar et al., 2022).

Considering that the remote sensing and observation data have the problem of teleconnection and couldn't represent the real flow system, without using any observation data, Wada et al. (2010) used a water-budget estimate method to compute the GWD. The global hydrological model PCR-GLOBWB was used in their study, which provided physical-process-based calculation method (Wada et al., 2010). It showed that North-East Pakistan and North-West India were hot spots of GWD in this world, ranging from 2 mm/yr to 1000 mm/yr. (Wada et al., 2010). However, this approach was intended to build a global model and didn't consider the real groundwater flow. In this way, it couldn't really explain the interior water system interactions in Indus basin and may tend to overestimate the GWD (Konikow, 2011).

By using a volume-based estimation method, de Graaf et al. (2017) built a global scale two-layer transient groundwater model, using PCR-GLOBWB and MODFLOW. The Indus Basin was also noted as one of the regions which experienced severe GWD worldwide. It showed that the North India and East Pakistan had up to 50 m cumulative GWD in 2010, resulted from human water use. However, it still suffered from several limitation such as coarse grid resolution and the not-fully-coupled integrated model. In

all, the broad estimation range of GWD in Indus Basin threatens the calculation of water availability here. Additional research endeavours are warranted to further explore this topic.

2.2 Model introduction

2.2.1 VIC-WUR model

VIC-WUR is a grid-based semi-distributed macroscale hydrologic model which can simulate the human impact on water resources in regional and global scale (Droppers et al., 2020). It is based on the Variable Infiltration Capacity model version 5 (hereafter refers as VIC-5) which simulates the full water and energy balance, using the method from the original VIC model developed by Liang et al. (Liang et al., 1994; Droppers et al., 2020). VIC model was originally designed as a land-surface model and already coupled to the atmosphere (Liang et al., 1994). The model simulated land-atmosphere fluxes, and the water and energy balance at the land surface, at a daily to sub-daily timestep. After decades of improvement and versions development, it has been successfully applied in climate change research, hydrological studies and water availability evaluation work in different regions of the world (Dan et al., 2012; Wang et al., 2012; Droppers et al., 2020; Gou et al., 2020). Recently, the newly developed version VIC-WUR extended several modules based on VIC-5 to simulate human impacts on water resources, which includes integrated routing, surface and groundwater use for irrigation, domestic, industrial, energy and livestock, environmental flow requirements and dam operation (Figure 4) (Droppers et al., 2020). It enabled VIC to study the impacts of both climate change and anthropogenic impacts on local region water scarcity (Droppers et al., 2020).

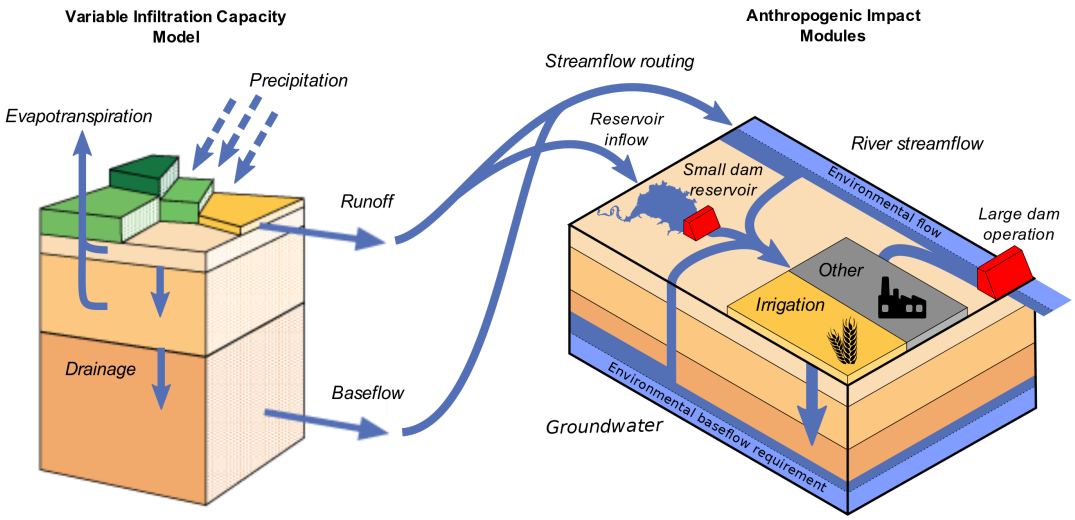

Figure 4 VIC-WUR model design

For each module, VIC-WUR has its well-developed calculation process. Integrated routing is one of the most important sectors in VIC-WUR as it produces the river

streamflow. It simulates runoff sequentially each timestep by using a routing module based on equations proposed by Lohmann et al. (1996). Also, it allows routing inflow forcing data to provided additional water inflow to specific cells, which reserves the possibility to couple with groundwater models. Moreover, VIC-WUR simulates water withdrawal, consumption and return flow for all sectors. Water demand of these sectors is provided as forcing data in the state file. Streamflow withdrawals are abstracted from grid cell discharge, while reservoir withdrawals stem from small dam reservoirs. Groundwater withdrawals are abstracted from the third layer of soil moisture, and the allocation of surface water withdrawals between river streamflow and small reservoirs is determined based on water availability (Droppers et al., 2020). Environmental flow requirements are used to constrain the water withdrawals, in terms of surface water and groundwater separately. Dam reservoirs is made distinct between 'small' and 'large' ones which locate in one grid cell or river cells (Döll et al., 2009). For crop growth, it is modelled by the WOFOST crop model (Droppers et al., 2022).

2.2.2 MODFLOW6 model

MODFLOW (Mcdonald & Harbaugh, 1984) is a modular hydrological model developed and maintained mainly by USGS. It was originally designed as a groundwater flow calculation program written in Fortran77 which is solely able to simulate groundwater flow (Wang et al., 2008). It has become the most widely used groundwater flow model in this world since early 1990s (Langevin et al., 2017). It included capabilities to resolve several hydrogeological problems and apply in different situations, such as solute transport, saltwater intrusion, parameter estimation, etc. (Harbaugh, 2005). It can numerically solve the three-dimensional groundwater flow equation using a finite-difference method (Xu et al., 2012), which could construct 2-D or 3-D groundwater models to resolve groundwater many quantity and quality problems (Khadri & Pande, 2016). MODFLOW6 is the newest version which develops a new framework that supports many of the functions that have been implemented in the MODFLOW variants, such as unstructured grids, local grid refinement, and parallelization capability of simulating multiple models at the same time using the Message Passing Interface (Langevin et al., 2017). This kind of change allows MODFLOW6 to couple with other hydrologic models (Langevin et al., 2017).

MODFLOW6 encompasses a range of packages designed to facilitate the characterization and simulation of groundwater flow system. The BAS6 package serves the purpose of delineating essential data, such as cell locations and initial hydraulic head values across the model domain. The DIS package is utilized to define the spatial discretization of the model domain, including parameters such as the number of rows and columns, cell dimensions, and temporal discretization. Additionally, the LPF and NPF packages are used to assign hydraulic properties to individual nodes and compute inter-cellular flow, encompassing attributes like hydraulic conductivity, horizontal and vertical anisotropy. For the delineation of specified head boundaries, the CHD package is deployed to simulate time-variant head conditions across stress periods. Similarly, the RCH package is utilized to represent recharge processes distributed over the model's

surface for specified flux boundary conditions. The WEL package is employed to model specific fluxes into individual cells from their respective surfaces. Furthermore, the EVT package is utilized to simulate head-dependent fluxes exiting the model surface. The RIV package plays a crucial role in defining and simulating flux boundaries associated with river systems. Finally, the OC package is utilized to designate the output variables, such as hydraulic head, drawdown, or budget data, to be printed or saved during the simulation process. In this study, these packages are all called and set manually to meet the different objectives.

Ch3 Methodology

3.1 Modelling approach

To answer the research questions and accomplish the objectives of this research, based on the information from the preliminary literature review, the hydrologic model and groundwater flow model of Indus Basin were built first by using VIC-WUR and MODFLOW6, respectively. Secondly, the groundwater model was coupled to the surface water model in offline way. VIC-WUR and MODFLOW6 were run independently for all stress periods, taking the outputs of river discharge and groundwater recharge from VIC-WUR as the inputs in MODFLOW6. Next, the two models were composited and coupled in partially online and fully online ways. It was realized by attaching the groundwater model built by MODFLOW6 to the bottom of the hydrologic model built by VIC-WUR. More specifically, there were two critical connections between the two models. In VIC-WUR model, it simulated surface and subsurface processes at each timestep to supply inputs of groundwater recharge and surface runoff to the MODFLOW6 model. Conversely, the MODFLOW6 model calculated capillary rise flux into the vadose zone and groundwater baseflow, contributing to total river discharge, which was then fed back into the VIC-WUR model. The model was run from January 1968 to December 2000, in total 396 time periods. The resolution of the model was 5 arcmin (approximately 10×10 km at the equator). More details are given in this chapter.

3.1.1 Coupling scheme

Coupling was classified into two main modes: offline coupling and online coupling. Offline coupling involved the independent execution of two models without mutual feedback during the entire simulation process. Specifically, the VIC-WUR model was initially run for the total stress periods, generating outputs such as river discharge, groundwater recharge, and human impact groundwater abstraction need when necessary. These outputs served as inputs for MODFLOW6, which subsequently ran for all stress periods. On the other hand, online coupling entailed the sequential execution of VIC-WUR and MODFLOW6 within a single stress period. For each stress period, MODFLOW6 utilized outputs from VIC-WUR as inputs, and concurrently, VIC-WUR incorporated outputs from MODFLOW6 to update its inputs. This dynamic interaction characterized the online coupling approach, where the models iteratively exchanged information to improve the authenticity of the simulation (Figure 5).

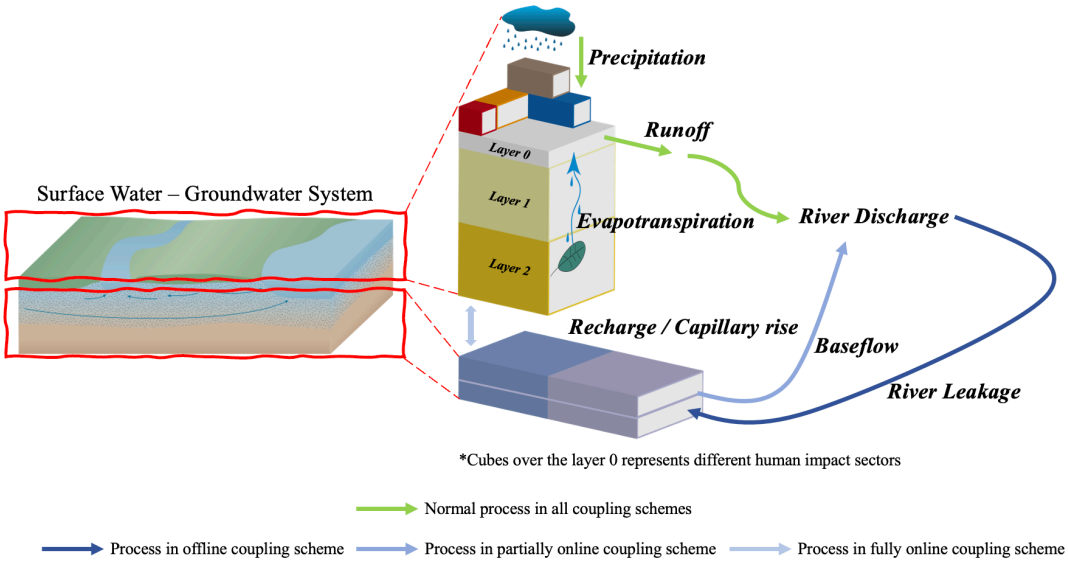

Figure 5 The coupling model design of this study

Under a technical context, the interaction between VIC-WUR and MODFLOW6 involved two distinct mechanisms (Figure 6). The first mechanism is the infiltration-capillarity system. Upon rainfall reaching the ground, a portion infiltrates into the soil, and some is intercepted by vegetation. In instances where the soil's infiltration capacity is surpassed, inland overflow occurs. Within the groundwater system, when the water table intersects the bottom of the unsaturated zone, capillary rise ensues, and vegetation roots extract water to the ground. VIC-WUR computes surface recharge to groundwater by precipitation. Through the incorporation of an additional evapotranspiration package in MODFLOW6, capillary rise to soil moisture is calculated. The second mechanism is the leakage-baseflow system. River leakage involves the infiltration of water from a river into the subsurface, replenishing groundwater. This phenomenon occurs as water from a surface water body permeates through the riverbed, banks, and into the underlying soil and rock layers. Baseflow, representing the steady and slow streamflow, is primarily sustained by the gradual release of groundwater. This flow persists between precipitation events. If the groundwater level exceeds that of the river, baseflow becomes significant, recharging the river. In MODFLOW6, the presence of baseflow is indicated by a negative computed groundwater discharge, while positive values signify river leakage. In the following analysis, to align with the total river discharge, positive values represent groundwater discharge, while negative values represent river leakage.

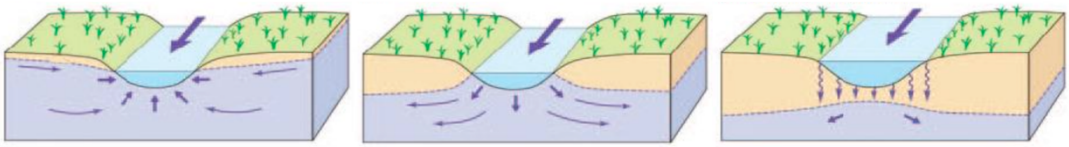

Figure 6 Surface water-groundwater interactions (Winter et al., 1998)

3.1.2 Conceptual model

Based on the available data, the aquifer was conceptualized as a quasi-three-

dimensional (quasi-3D) transient two-layer groundwater system. The delineation of the boundary was determined by the actual shape of the basin. In MODFLOW6, inactive land cells and ocean cells were indexed as 0 and -1, respectively. Active boundary cells were designated as 1, while the cells at the interface between land and ocean were assigned a value of 4. Inner active computed cells were all set to 2. The visualization of idomain can be found in Appendix A. A time-variant constant head boundary was employed in this modelling work, wherein for each stress period, a series of GWL datasets containing two layers were input into the model boundaries. The groundwater level data were computed based on the groundwater depth and DEM data, from Inge de Graaf's global groundwater model (de Graaf et al., 2015). Details are as follows:

$$\mathrm{GWL}_{i,j,k,l}|_{j\neq 0} = \mathrm{DEM}_{k,l} - \mathrm{GWDE}_{i,j,k,l} \quad (1)$$

Where GWL_i is groundwater level (m). DEM is ground elevation (m). GWDE is groundwater depth (m). i is layer index. 1 is top layer and 2 is bottom layer. j is stress period index, with a total number of 396. k is latitude index, ranges from 1 to 180, l is longitude index, ranges from 1 to 204. In this way, the groundwater level data of each grid cell in each layer for the whole stress periods were obtained. The value was assigned to the boundary of each layer in each stress period to run a transient model. Furthermore, by executing a steady-state model utilizing the average GWL as the starting head, the steady-state GWL could be determined and designated as the initial head in the model:

$$\mathrm{GWL}_{i,j,k,l}|_{j=0} = \mathrm{GWLSS}_{i,k,l} \quad (2)$$

Where, GWLSS is the steady-state groundwater level.

In this model, sources and sinks included groundwater recharge, river discharge and evapotranspiration, used for representing capillary rise, which were also time-variant data. Groundwater recharge and river discharge were computed by VIC-WUR in each stress period. River discharge was extracted from the VIC-WUR output, along with an average input river discharge, to compute river characteristics utilized in the model. These characteristics encompass width, slope, stage, bottom, and conductance. The stage and bottom were set based on different river width, which are drains and large rivers. For all the rivers and drains, the width is set to no less than 0.5 m and computed as follows:

$$\mathrm{RW} = \max\begin{cases} 4.8 \times \sqrt{\mathrm{Q_{avg}}} \\ 0.5 \end{cases} \quad (3)$$

Where, RW is river width (m), Q_{avg} is the average river discharge (m^3/s). For the river conductance:

$$\mathrm{RC} = \begin{cases} \frac{1}{\mathrm{RR}} \times \mathrm{RW} \times \sqrt{2\mathrm{CA}}, \mathrm{RW} \geq 30 \\ 0, \mathrm{RW} < 30 \end{cases} \quad (4)$$

RC is river conductance with flux unit. RR is river resistance which was set to 1. CA is

the cell area (m^2). For drains, the width and conductance were set as follows:

$$\mathrm{DW} = \max\begin{cases}10\\ \mathrm{RW}\end{cases} \tag{5}$$

$$\mathrm{DC} = \begin{cases}\frac{1}{\mathrm{RR}} \times \mathrm{DW} \times \sqrt{2\mathrm{CA}}, \mathrm{RC} = 0\\ 0, \mathrm{RC} \neq 0\end{cases} \tag{6}$$

Where DW is drain width (m), DC is drain conductance with flux unit. Then, the final river conductance for all rivers and drains is expressed as:

$$\mathrm{RDC} = \begin{cases}\mathrm{RC}, \mathrm{RC} > 0\\ \mathrm{DC}, \mathrm{RC} \leq 0\end{cases} \tag{7}$$

The evapotranspiration used to represent capillary rise requires values of the elevation of the ET surface (m), maximum ET flux rate (m/d) and ET extinction depth (m). MODFLOW6 takes these data to calculate if the evapotranspiration (capillary rise) would occur in this grid and the relative amount in each stress period. This portion of water will be lost from the entire model and will not be replenished.

3.1.3 Parameterization

The Indus Basin was formed approximately 15 million years ago due to the uplift of the Himalayas, the load on the lithosphere, and the subsidence of the Indian continental plate (Bonsor et al., 2017). Across the majority of regions, the aquifer system is covered by unconsolidated alluvium. The sediment thickness is substantial, boasting high hydraulic conductivity ranging from 20 m/d to 50 m/d (Shamsudduha et al., 2011). The specific yield is in the range 0.1 – 0.15 (Bonsor et al., 2017). In numerous sections of the basin, groundwater extraction is concentrated within the upper 200 m of these sediment layers. (Bonsor et al., 2017). The river streams in the Indus Basin flow from the northeast mountainous area to the southwest plain and eventually into the Arabian Sea of the Indian Ocean. The mean annual precipitation in the Indus Basin is 365 mm. The upper Indus region receives approximately 500 mm/year, while the lower basin receives slightly less, just under 300 mm/year.

Based on the available information, aquifers were distinguished into confined and unconfined layers based on the information of grain sizes (de Graaf et al., 2017), with specific storage and specific yield values allocated accordingly to each type of aquifer. A uniform specific yield of 0.15 was assigned to all unconfined aquifers. The specific storage spanned from 0.11 to 0.36, as depicted in Figure 7 (left). The aquifer thickness was delineated by a stratified structure, wherein the upper layer accounted for 10% of the total thickness and the remainder formed the lower aquifer. The horizontal hydraulic conductivity ranged approximately from 0 to 30 m/d, as shown in Figure 7 (right). The vertical hydraulic conductivity was set to 10% of the horizontal value.

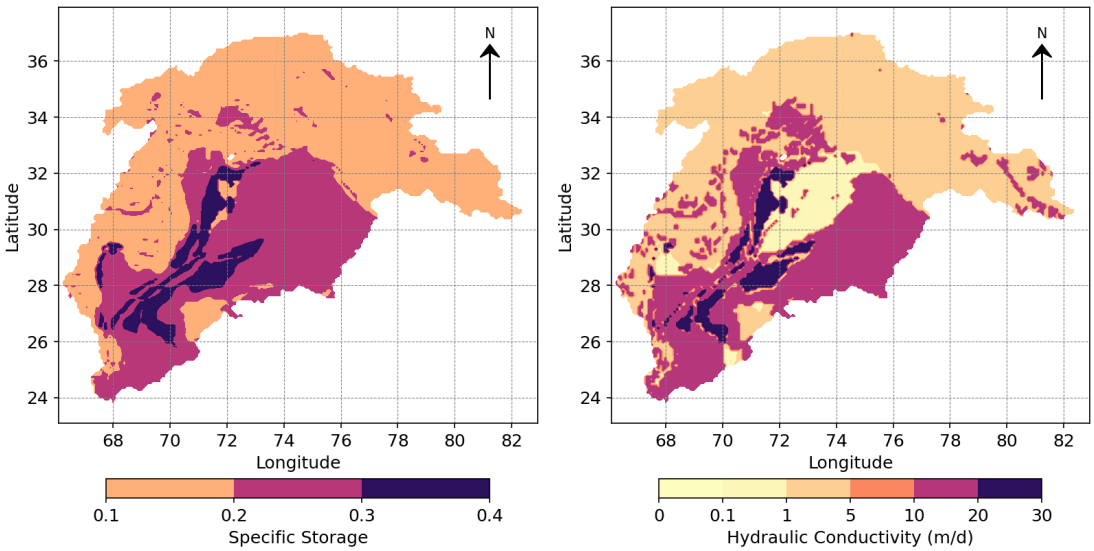

Figure 7 Settings of specific storage (left) and hydraulic conductivity (right) in the model

3.2 Data

3.2.1 Data processing

All the data used in this study are based on the global transient groundwater model developed by Inge de Graaf in 2017 (de Graaf et al., 2017). They were extracted from the global dataset and made slight adjustment including reversing the direction, defining the boundary, coding the index, calculating groundwater level for initial and boundary condition, etc. Full input list can be found in Appendix B. The main input datasets and their uses are listed below in Table 1.

Table 1 Main input datasets and their uses

Dataset	Use
demfrom30s.nc	Indus Basin terrain
damc_ave.nc	Initial aquifer depth
lkmc_ave.nc	To define hydraulic conductivity
Qbank_new_average.nc	To calculate river width
mindem_05min.nc	DEM used to define river head
conflayers4.nc	Separate confine and unconfine layers
kl1B_ave.nc	To define top layer hydraulic conductivity
StorCoeff_NEW.nc	Specific yield
boundary.nc	To define the boundary

3.2.2 Unit conversion

VIC-WUR typically produces output related to soil moisture, runoff, and other surface water-related variables, whereas MODFLOW6 provides information on hydraulic conductivity, initial groundwater levels, boundary conditions, etc. Occasionally, there are mismatches in units between the two models, requiring unit conversion before modelling. References for unit conversion of key parameters are provided in Table 2 below.

Table 2 Unit conversion table

VIC-WUR		**MODFLOW6**	
Parameters	**Unit**	**Parameters**	**Unit**
Precipitation	mm/month	Recharge	m/day
Evapotranspiration	mm/day, m/day		
Time	month	Time	day
Soil moisture	mm	Hydraulic conductivity	m/s
		Hydraulic head	m
		Water table depth	m
River discharge	m^3/s	River stage	m
		River bottom	m
		River conductance	m^2/day

3.3 Input settings

All inputs were read simultaneously prior to the commencement of the first stress period, followed by a spatial data flip. This is necessary due to the different data read methods employed in VIC-WUR and MODFLOW6, which have different data origins. Both models saved results at each stress period and subsequently updated to another under POC and FOC. The simulation settings for NatCon and HumanCon were largely identical, with the exception that in HumanCon, VIC-WUR was configured to generate the 'NONRENEWABLE_WITHDRAWAL' variable to represent human water use in each stress period. Here visualizes the recharge input as a sample.

The recharge rate has significant seasonal changes. During autumn and winter, the recharge rate is notably low, with only minimal recharge occurring in the high mountain areas. In contrast, during spring and summer, while the plain areas maintain a relatively low recharge rate, the upper basin experiences a period of high recharge, with the maximum value reaching 85.64 mm/month. The human activities almost don’t affect

the recharge rate to groundwater. Same with that in OFC-NatCon, there are much more recharge in spring and summer but fewer in autumn and winter. The value ranges from 0 mm/month to 85.79 mm/month, only a slightly higher than that in OFC-NatCon.

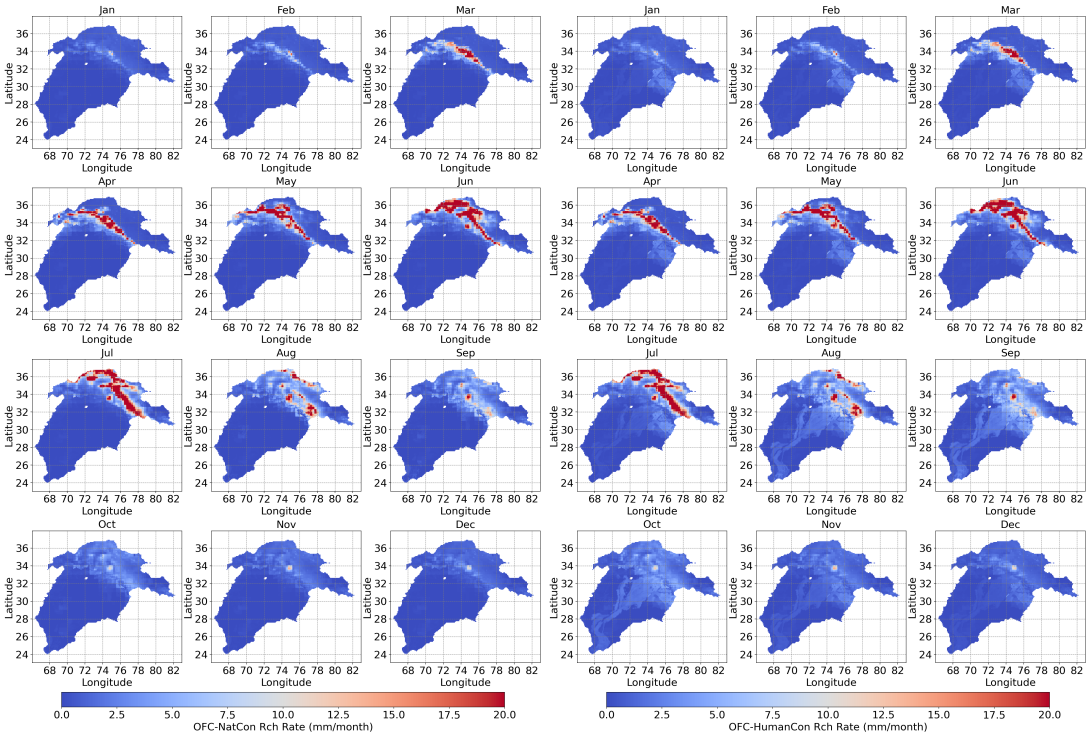

Figure 8 Monthly variation of recharge rate under OFC (left: NatCon; right: HumanCon)

Ch4 Results Analysis

This chapter presents the results of the study, encompassing offline coupling (OFC), partially online coupling (POC), and fully online coupling (FOC). Throughout the analysis, the top layer represents the analysed groundwater layer, while the bottom layer is utilized solely for simulation purposes and is excluded from the analysis. In OFC, both NatCon and HumanCon are considered in model execution. The analysis consists of the behaviours of GWL, recharge rate, and baseflow across different coupling schemes and conditions, exploring both spatial and temporal aspects. Each subsection offers detailed insights. To mitigate the influence of relatively ambiguous initial conditions and to better showcase the results, the analysis period is set from January 1970 to December 1999, spanning 30 years and 360 time periods.

4.1 Naturalized Condition – NatCon

The naturalized condition (NatCon) was configured to mirror the influence of historical climate variations during the simulation period (1968 – 2000) within the Indus Basin. In this setting, all three coupling schemes - OFC, POC, and FOC - were systematically applied to comprehensively capture the dynamics of the system. The analysis includes the variations of GWL and baseflow, encompassing groundwater discharge and river leakage, through an exploration of long-term monthly averages (hereafter refers as ltma) and seasonal behaviours. By analysing these hydrological characteristics across different coupling schemes, a comprehensive understanding of the basin's hydrological responses to historical climate fluctuations was attained.

4.1.1 Offline Coupling

Under NatCon, the offline coupling model under naturalized condition (hereafter refers as OFC-NatCon) was first constructed and simulated. Given the absence of in-situ real-time observation GWL data, an initial steady-state model was executed to acquire the GWL as the starting condition for subsequent simulations. This was achieved by utilizing the computed average GWL spanning the period between 1968 and 2000 as the initial head in the steady-state model (Figure 9). The GWL exhibits a notable elevation gradient, with higher levels observed in the northeast Himalayan mountainous area and lower levels in the southwest plain and coastal regions. Across the majority of the Indus Basin, the GWL range from 0 to 2000 m. However, in the upper mountainous areas, the GWL can reach peaks exceeding 5000 m.

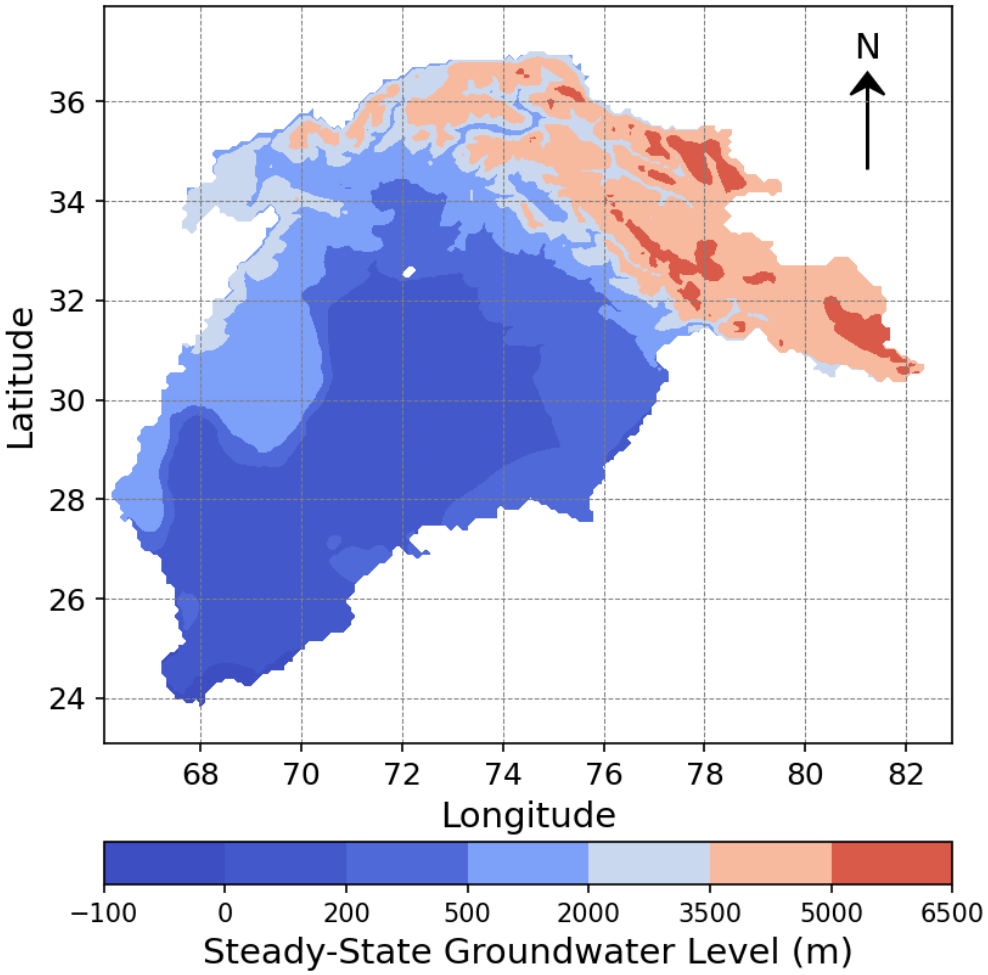

Figure 9 Steady-state groundwater level under OFC-NatCon

By taking the steady-state GWL as the initial head, the transient model showed variations of characteristics of surface water and groundwater. Due to the significant variation in surface elevation within the Indus Basin, an assessment of the temporal variation of GWL was conducted. To achieve this, a total of six random cells were selected, comprising two from the upper, middle, and lower basins respectively, as shown in Figure 10. The indexes listed in the figure correspond to the cell row and column indices in MODFLOW6, denoting the precise locations of cells. Specifically, U1 and U2 denote cells in the upper basin, M1 and M2 represent cells in the middle basin, and L1 and L2 represent cells in the lower basin. These cells encompass river, plain, and mountain regions, providing a comprehensive perspective on the variations in GWL.

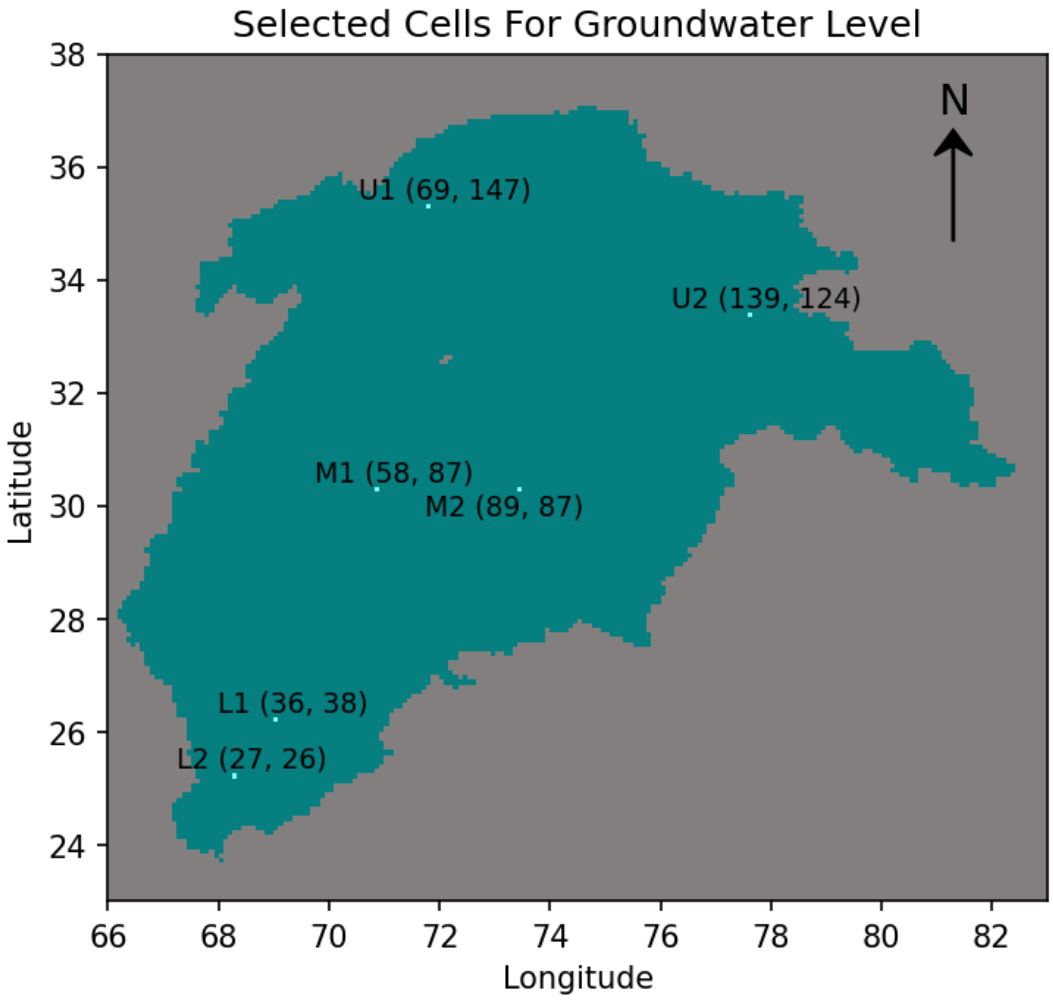

Figure 10 Selected cells for groundwater level analysis

The plotted time-series in Figure 11 presents the fluctuations in GWL at six cells under NatCon. Throughout the regions depicted, discernible seasonal patterns emerge, indicating regular changes in GWL over the course of a year. These cells were specifically chosen from diverse regions of the basin, and as such, each of the six exhibits a unique pattern of GWL variation. Notably, Cell U1 and U2 in upper basin exhibits more pronounced variations compared to the middle and lower basins. The disparity between the highest and lowest GWL reaches 5.08 meters in Cell U1 and 0.02 meters in Cell L1. Among the six cells, three out of four cells in the upper and middle basin exhibit a decrease in GWL, while the remaining cells show a slight increase in GWL. Additionally, for cells situated near rivers or drains, the seasonal variation in GWL is more pronounced compared to others. Conversely, other cells tend to align with the recharge pattern and terrain variation more closely.

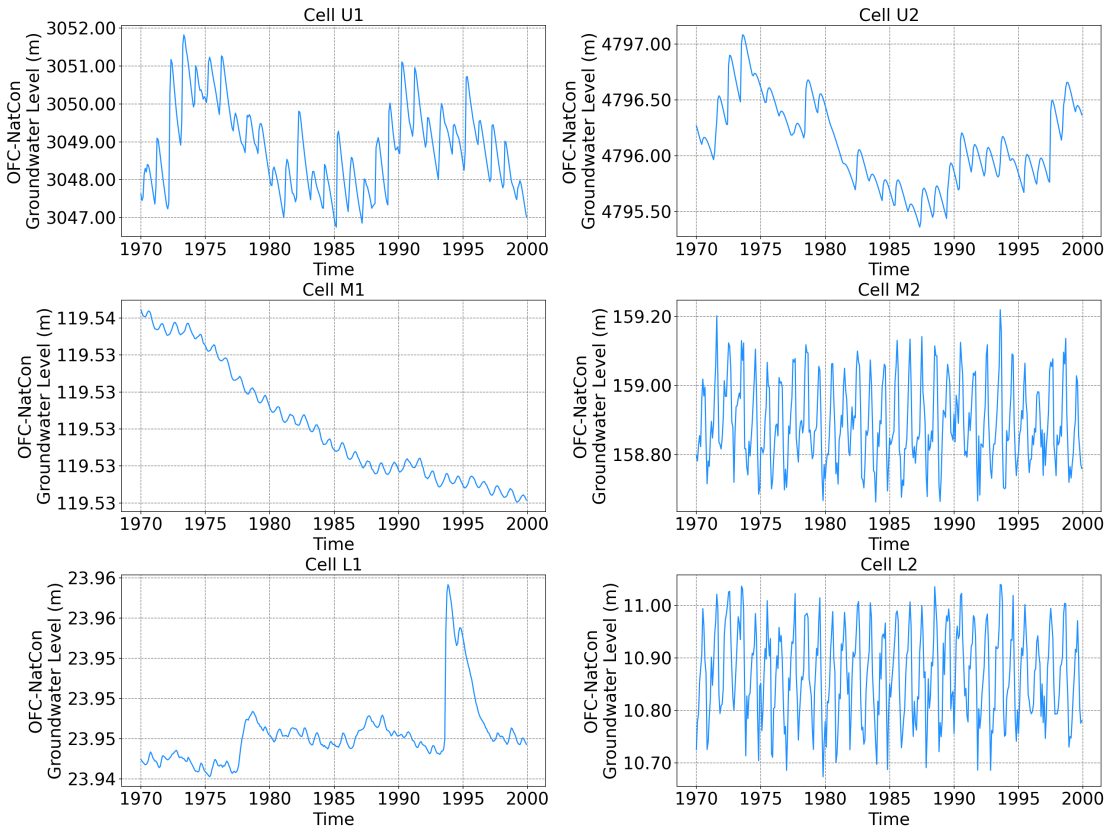

Figure 11 OFC-NatCon six cells time-series plots of GWL

The long-term monthly average GWL data reveals seasonal fluctuations (Figure 12). On a comprehensive scale, the seasonal fluctuations in GWL are not particularly pronounced. The maximum difference in GWL reaches 1.46 m, observe in cell U2, while the minimum difference is merely 0.0004 m, noted in cell M2. This suggest that under natural conditions, the groundwater system of the Indus Basin remain relatively stable. Among the six cells, five consistently display their highest GWL during the summer and autumn months, from July to October. Conversely, only one cell in the upper basin exhibits its peak in May. Additionally, four cells showcase their lowest levels during winter, while two experience this during summer. Significantly, clear fluctuation patterns are discerned in the plotted data, suggesting inherent natural fluctuations. No matter if the water levels are high or low in any season, the GWL at the six points always shows a pattern of ups and downs. There are no instances where GWL consistently decrease or increase throughout the twelve months. This pattern aligns with the behaviour of GWL observed in most regions of this world under natural conditions.

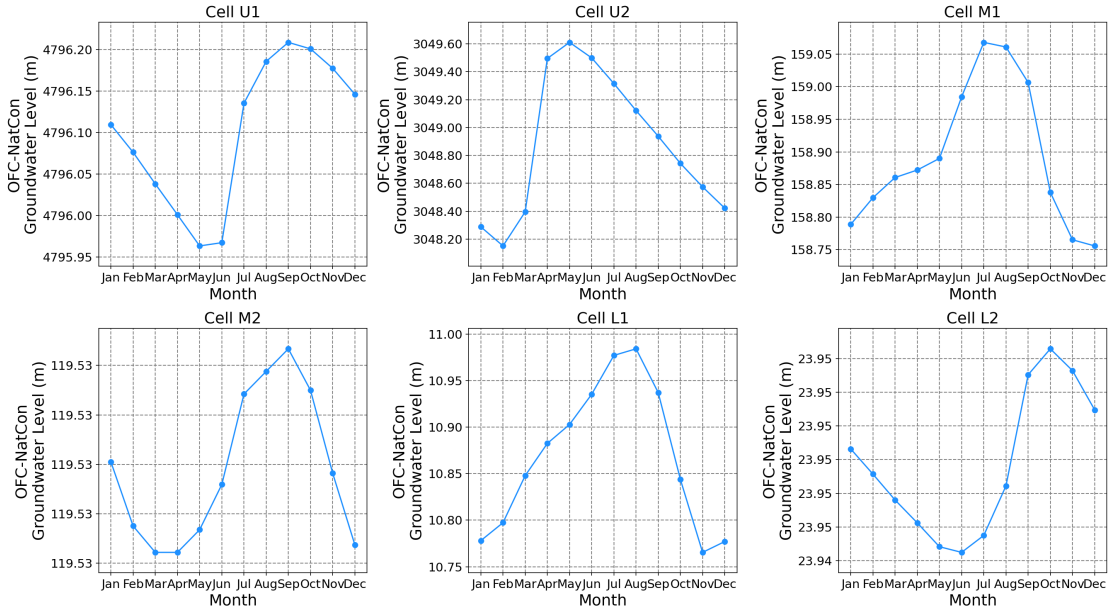

Figure 12 OFC-NatCon six cells monthly variations of GWL

Under the OFC-NatCon simulation, the GWL experience a very gradual decline. In fact, more than half of the basin show not a deficit but rather a slight increase in GWL due to the recharge and low hydraulic gradient, especially in the lower basin. Within the areas where experience GWL drawdown, more than 90% varies only within 1 m, almost all in the upper mountainous area and near mid-lower river channels (Figure 13). However, it's worth noting that only a minority of cells exhibit a significant decrease in GWL in the high mountainous regions. Given the low river runoff observed in these areas, this phenomenon can be interpreted as groundwater passively replenishing to river flow, thus contributing to a relatively noticeable decline in GWL. This interaction between groundwater and river flow underscores the complex dynamics of hydrological processes in mountainous terrains. In the vicinity of rivers in the middle to lower reaches, it is evident that GWL show little to no decline, with some areas even experiencing an increase. This phenomenon can be attributed to the fact that in the downstream areas, river levels are typically higher than GWL. Therefore, under natural conditions, rivers actively replenish groundwater.

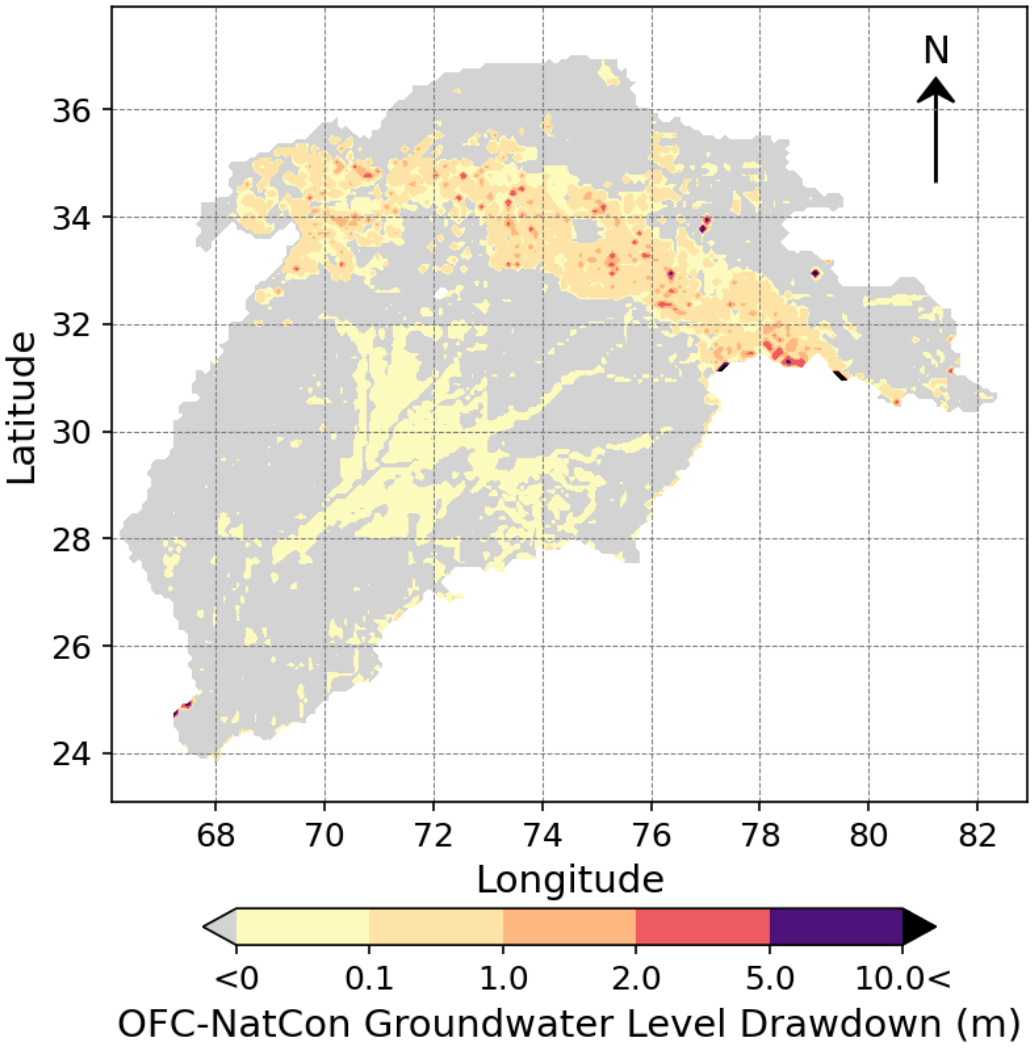

Figure 13 OFC-NatCon groundwater level drawdown

Apart from GWL, following each stress period simulation, MODFLOW6 generated the water budget within the model. This budget primarily mainly comprises the constant head budget, river budget, recharge budget, evapotranspiration budget, and storage budget. Here, particular attention is given to the river budget as it explains the interaction between surface water and groundwater most, which includes rivers and drains recharge to groundwater and baseflow from groundwater discharge specifically. The raw outputs were processed that the current positive value indicates groundwater discharge to the river, while negative values signify river flow leaks into the groundwater (Figure 14). The term 'baseflow' here is a general definition which includes groundwater discharge and river leakage. In Indus Basin, groundwater discharge is the predominant sector compared to river leakage. Remarkably, the total groundwater discharge over the analysis period is approximately 70 times greater than river leakage. Specifically, in the upper mountainous basin, groundwater discharge is consistently observed throughout the year. In contrast, in the mid-lower basin, river flow into groundwater predominantly occurs during spring and summer. Conversely, during autumn and winter, the river ceases to leak and instead accepts water flows from the groundwater aquifer.

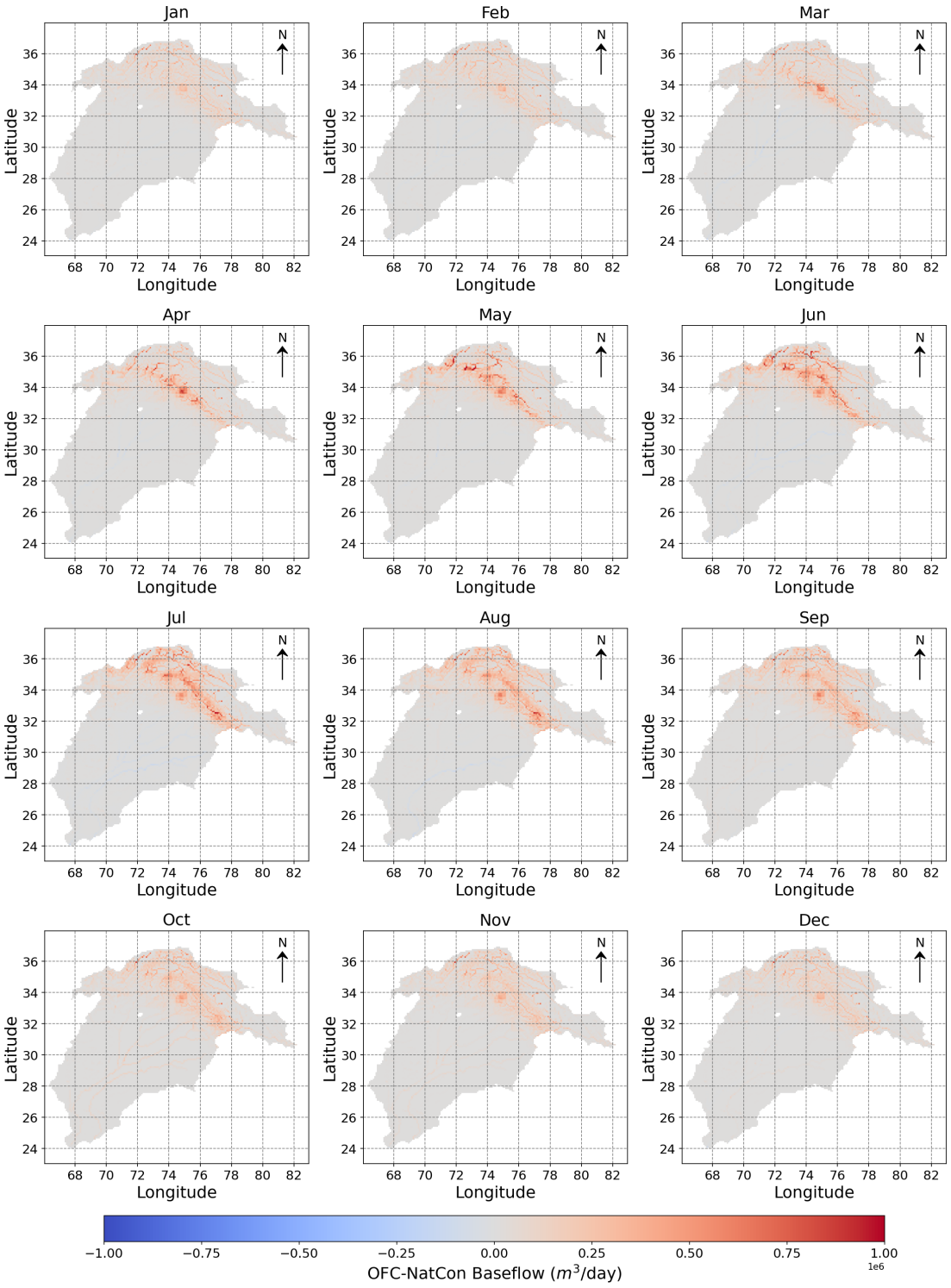

Figure 14 OFC-NatCon long-term monthly average baseflow

As baseflow predominantly occurs within or in close proximity to rivers and drainage channels, evaluating baseflow variations in areas lacking river flow is inappropriate. Therefore, another six randoms cells located in river were chosen, two from each region. These cells are indicted in Figure 15: U3, U4 represent upper basin cells, M3, M4 represent middle basin cells and L3, L4 represent lower basin cells.

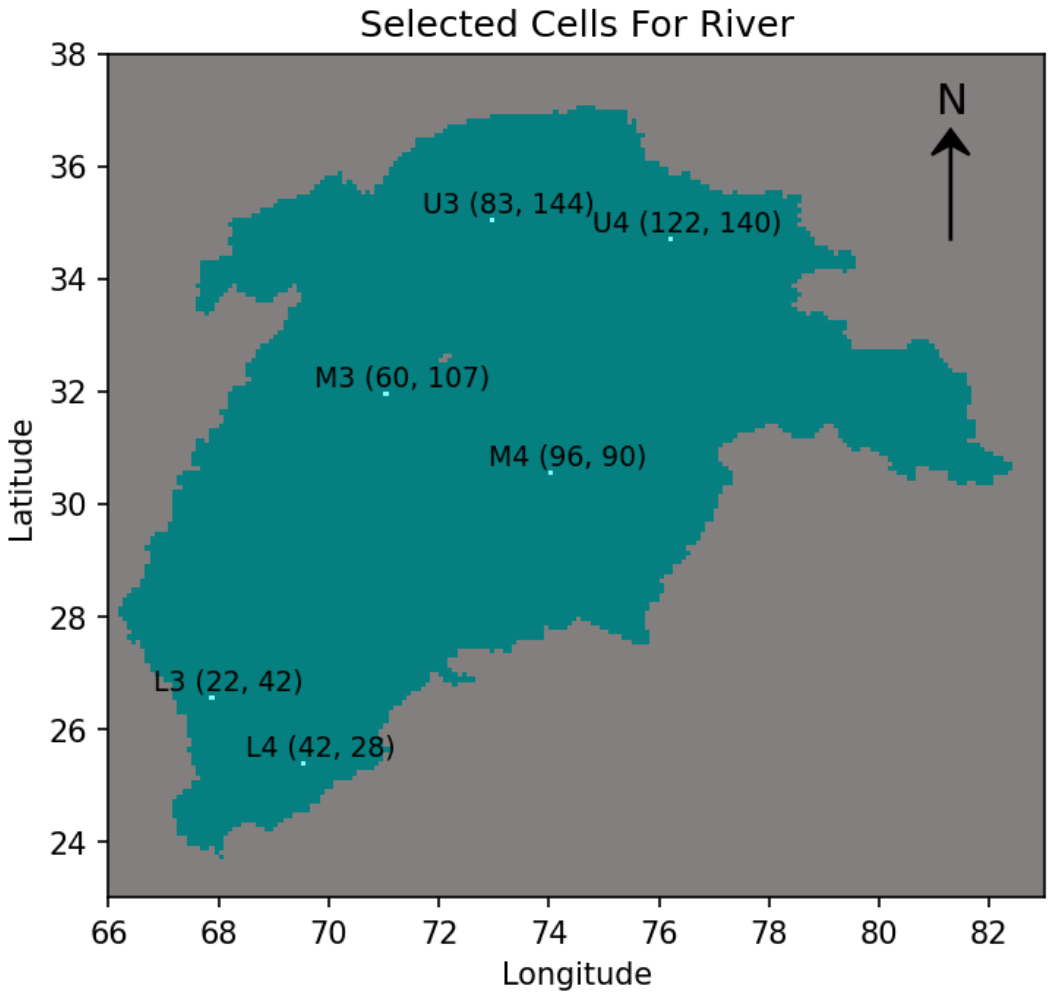

Figure 15 selected cells for river analysis

The time-series variation of baseflow exhibits distinct basin characteristics. All six cells exhibit clear interannual variation patterns, becoming less pronounced from the upper to the lower reaches. The characteristic feature is the alternating occurrence of high and low years in baseflow intensity (Figure 16). The cells in the upper basin consistently exhibit positive baseflow throughout the entire year among the six cells and have a more pronounced alternation between groundwater discharge and river leakage. In comparison, the middle and lower reaches of the basin exhibit smaller variations. Numerical comparisons provide a more intuitive understanding. Among the six cells, baseflow varies from approximately 63,457 m^3/day to 1,085,564 m^3/day in upper basin, -110,291 m^3/day to 313,820 m^3/day in middle basin and -172,864 m^3/day to 193,395 m^3/day in lower basin (Figure 16). The significant differences in baseflow across various regions of the basin highlight the heterogeneous nature of groundwater dynamics. While the upper basin shows a broader range of baseflow values,

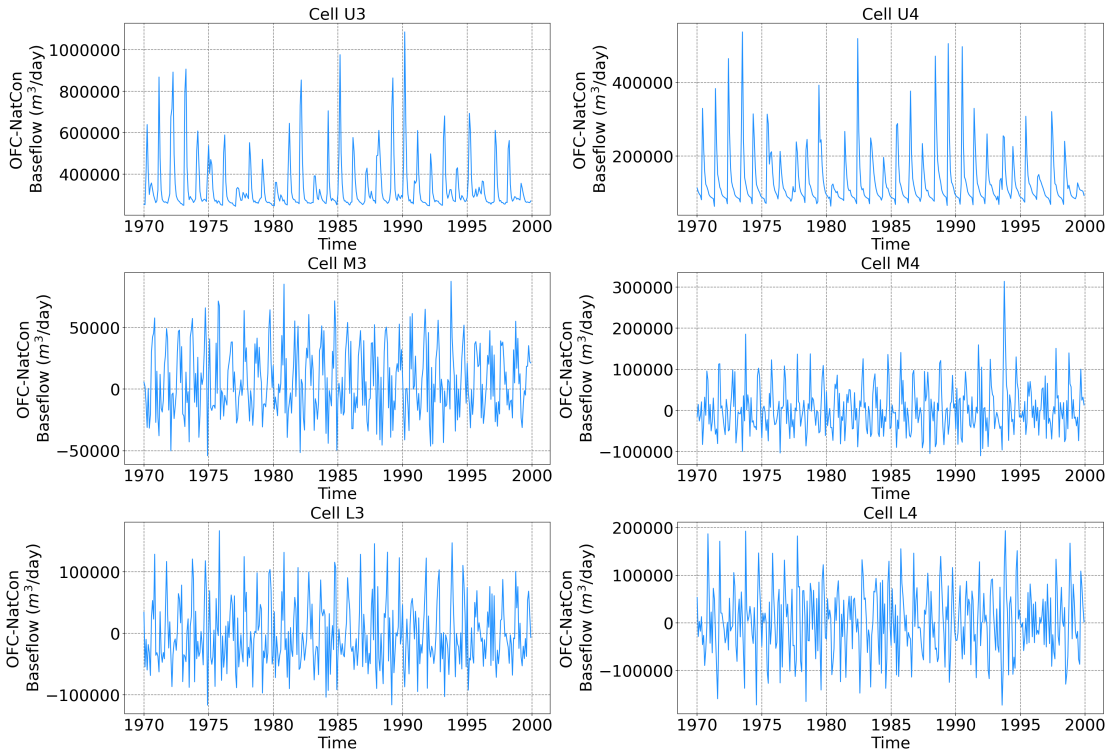

Figure 16 OFC-NatCon six cells monthly baseflow

Aggregating the time series data into monthly averages allows for the examination of the long-term monthly average of GWL and baseflow across the six river cells, revealing the correlation between these two aspects, as shown in Figure 17. Due to the long-term stability of river flow, the overall fluctuations in GWL across river cells are relatively small. Generally, they exhibit higher levels in summer and autumn, and lower levels in winter and spring. Compared GWL with baseflow, in the upper reaches, GWL and baseflow exhibit nearly identical co-variation trends, indicating that baseflow does not significantly affect GWL fluctuations in this region. However, in the middle and lower reaches, a starkly contrasting trend emerges. The GWL and baseflow exhibit opposite trends, attributed to the positive baseflow indicating groundwater replenishment to the river, resulting in a subsequent decline in GWL, and vice versa. This indicates that groundwater in the middle and lower reaches is more sensitive to changes in baseflow. Simultaneously, a hysteresis can also be observed. When baseflow initiates a change, GWL exhibit a lagged response, consistently peaking half a month to a month later than baseflow. This also demonstrates the self-regulating capacity of the groundwater system. Furthermore, due to variations in hydraulic gradients, topographical conditions, and primary sources of recharge, this capacity may differ, as evidenced in the upper, middle, and lower reaches.

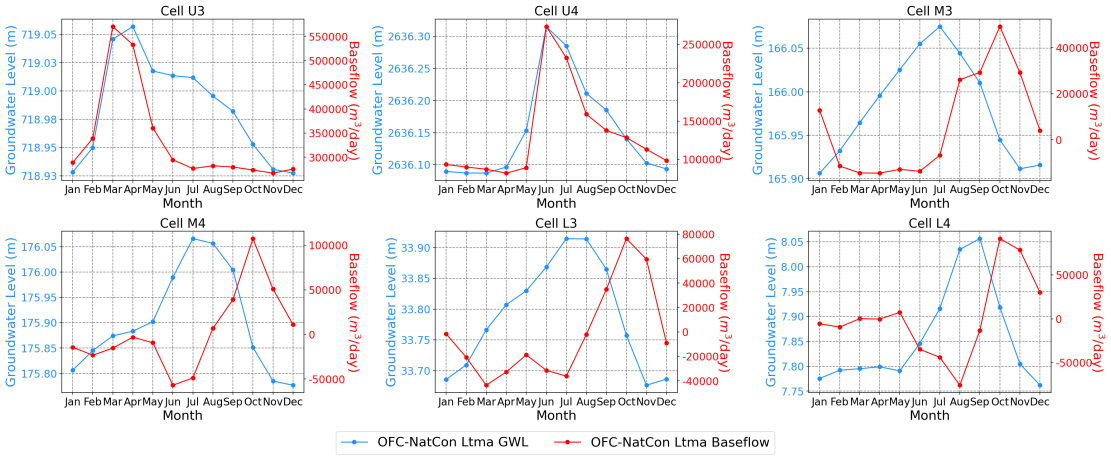

Figure 17 OFC-NatCon long-term monthly average GWL and baseflow

4.1.2 Online Coupling

The online coupling model under naturalized conditions was developed to improve the estimation of hydraulic characteristics. This encompasses two models: partially online coupling (POC) and fully online coupling (FOC), which respectively update baseflow and both baseflow and capillary rise during each stress period. Due to the similar trends observed in some results across the three coupling schemes (such as GWL), not all figures will be displayed here. Instead, only the most significant findings regarding the impact on baseflow will be presented. More detailed content and figures can be found in the discussion section.

The same six river cells were selected for analysis for ease of comparison with the previous sections (Figure 18). In POC, similar to OFC, baseflow in the upper reaches is entirely positive and exhibits the most pronounced interannual variation, ranging from approximately 77,355 m^3/day to 1,088,586 m^3/day. The baseflow variation in the middle reaches is relatively minor compared to the upper reaches, ranging from -80,993 m^3/day to 202,244 m^3/day. Additionally, there are no pronounced interannual variations here. Only in 1993-1994 was there a notably higher value, likely attributed to a sudden increase in recharge at that time. The baseflow variation in the downstream cells is overall more subtle, ranging from -178,103 m^3/day to 258,074 m^3/day. Additionally, there is an increase in river leakage in lower basin, while the proportion of groundwater discharge decreases. However, overall, groundwater discharge still far exceeds river leakage, which also indirectly indicates the substantial contribution of groundwater to river replenishment.

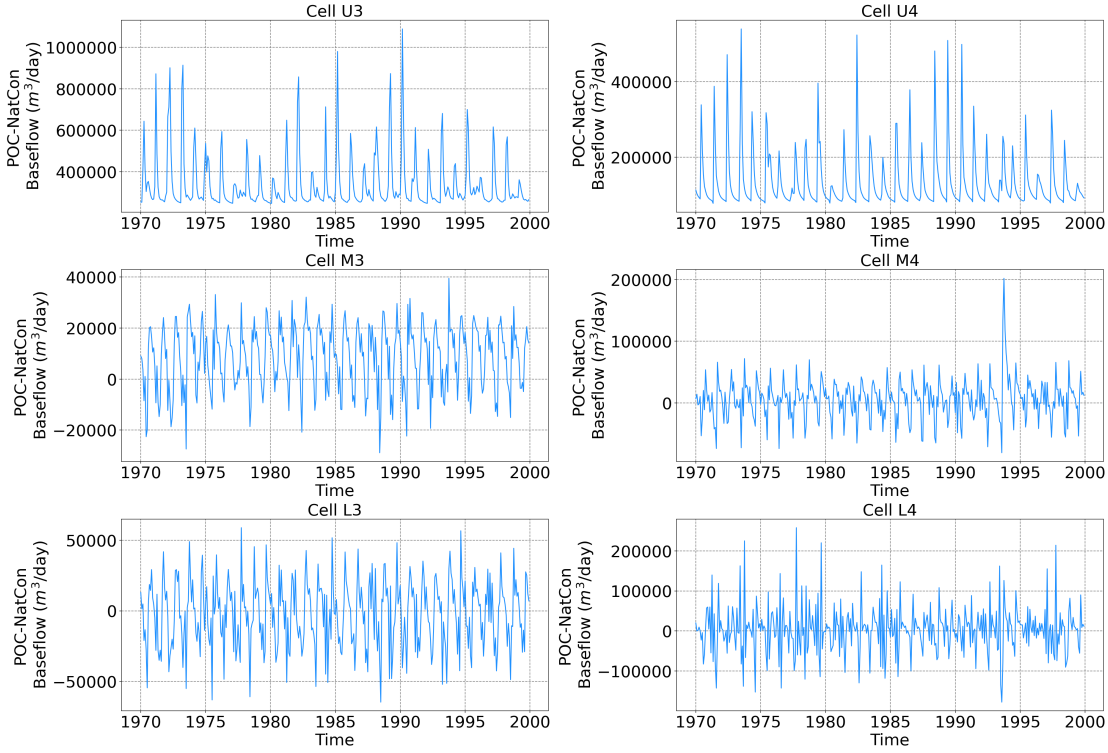

Figure 18 POC-NatCon six cells daily average baseflow

For long-term monthly average data, POC also exhibits similar trends to OFC, but with some differences in detail. In the rivers of the upper reaches, the co-variation trend between baseflow and GWL is more pronounced, with almost no hysteresis observed. However, for cells located on rivers in the middle and lower reaches, the reverse trend and lag effect between baseflow and GWL are more pronounced, as shown in Figure 19. The peaks of both variables clearly alternate, further indicating the high degree of connectivity between groundwater and rivers in the middle and lower reaches of the Indus Basin.

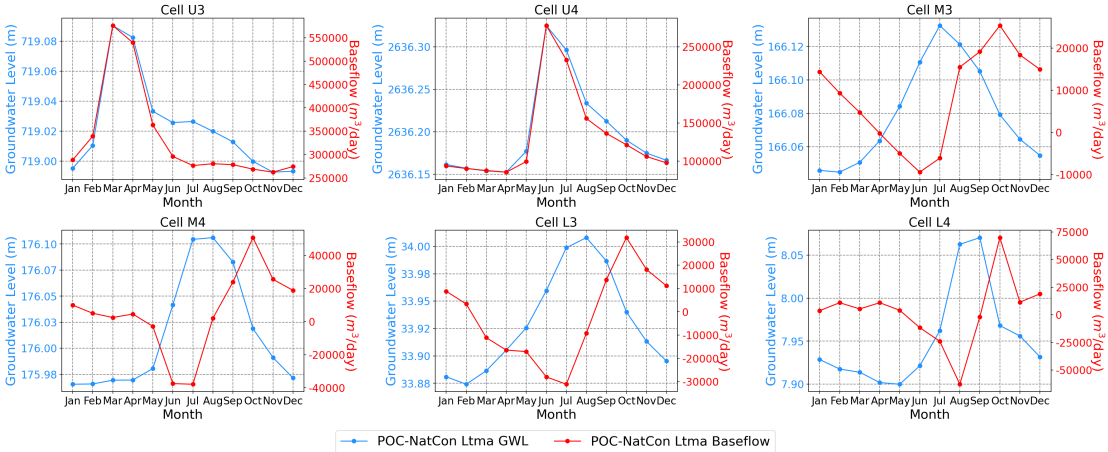

Figure 19 POC-NatCon long-term monthly average GWL and baseflow

Under POC-NatCon, while the general trend of overall baseflow resembles that under OFC, a more detailed analysis separates baseflow into groundwater discharge and river

leakage to illustrate their distinct behaviours. In general, the total groundwater discharge over the analysis period is 120 times greater than river leakage, bigger than the difference under OFC. The highest average groundwater discharge occurs in July with the value of 47,801 m^3/day and the lowest occurs in February with the value of 23,680 m^3/day. As shown in Figure 20 (left), in most part of the middle and lower basin, there's no groundwater discharge but only river leakage, which reveals the spatial variation of baseflow. The average groundwater discharge is 35,082 m^3/day, and the maximum value is 1,776,687 m^3/day, occurs in the upper mountainous area. This highlights the significant contribution of groundwater from mountainous areas to river flow. River leakage to groundwater primarily occurs during the summer months. Among all twelve months, July exhibits the highest average river leakage, amounting to 1,150 m^3/day, representing 2.4% of the average groundwater discharge for that month. October has the lowest average river leakage at 37 m^3/day, which is only 0.1% of the groundwater discharge for the same month, indicating a significant difference (Figure 20 (right)).

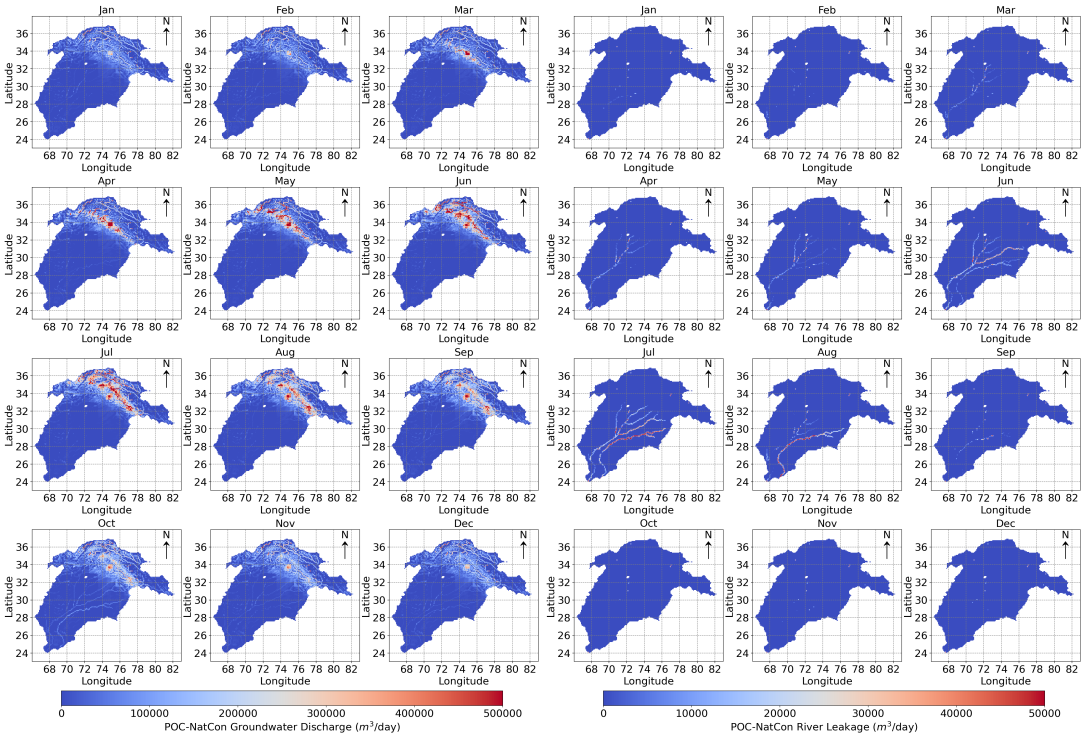

Figure 20 POC-NatCon long-term monthly average groundwater discharge (left) and river leakage (right)

FOC added capillary rise in the model, which was conceptualized as evapotranspiration in MODFLOW6. Under FOC, the trend of baseflow change is very similar to POC (Figure 21). Among the six river cells, baseflow varies from approximately 77,355 m^3/day to 1,088,568 m^3/day in upper basin, -80,837 m^3/day to 203,718 m^3/day in middle basin and -178,264 m^3/day to 260,322 m^3/day in lower basin. Considering that capillary rise occurs within a very limited range and involves relatively small quantities, it is reasonable to conclude that it would have minimal impact compared to the flow of baseflow. Exactly for this reason, the long-term average monthly baseflow under FOC

is almost indistinguishable from that under POC, as shown in Figure 22.

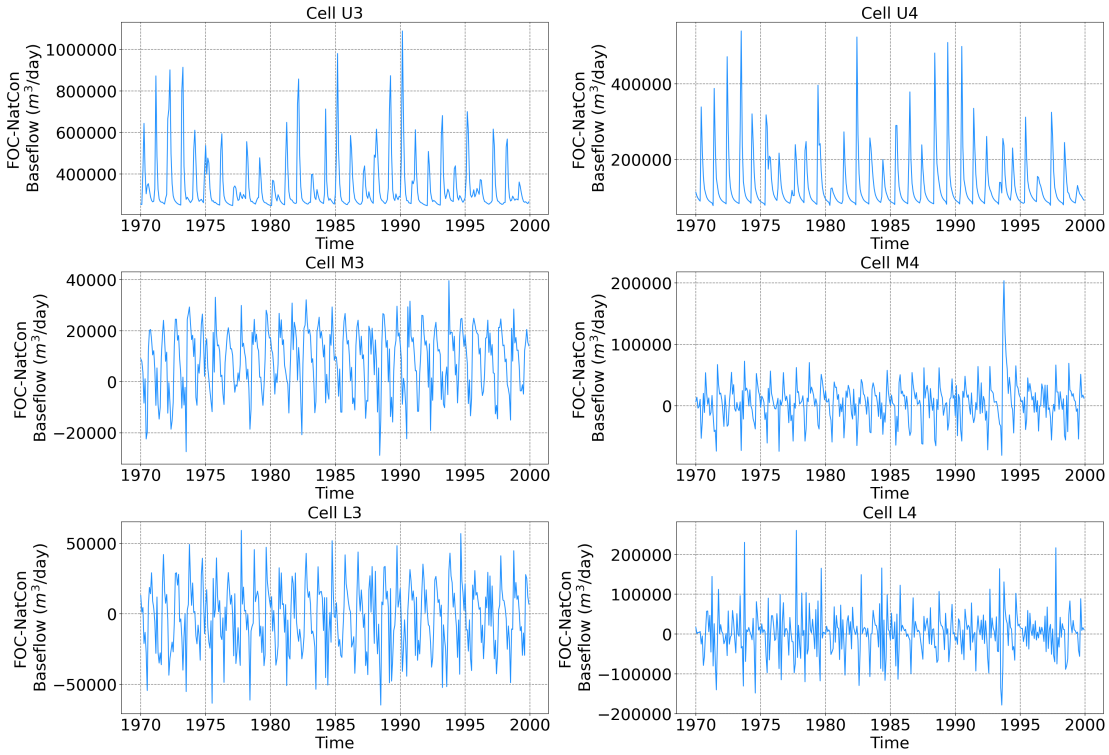

Figure 21 FOC-NatCon six cells monthly baseflow

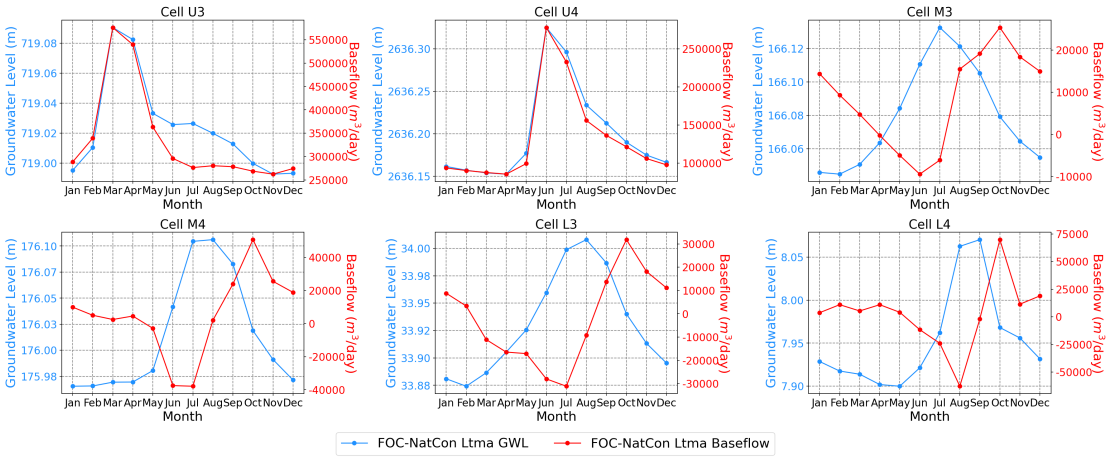

Figure 22 FOC-NatCon ltma GWL and baseflow

Under FOC-NatCon, the highest and lowest monthly average groundwater discharge are all slight lower than under POC, at a value of 47,650 m^3/day in July and 23,624 m^3/day in February, respectively (Figure 23 (left)). For single cell, the maximum groundwater discharge is 1,776,690 m^3/day, occurs in the upper mountainous area. The river leakage under FOC is virtually identical to that under POC. The peak of the river leakage under FOC also occurs in July at an average of 1,130 m^3/day and October has the lowest average river leakage at 37 m^3/day (Figure 23 (right)). This also reflects the contribution of capillary rise: its impact is more significant and direct on groundwater discharge, but due to the hysteresis and complexity within the groundwater system, this

effect does not propagate to river leakage.

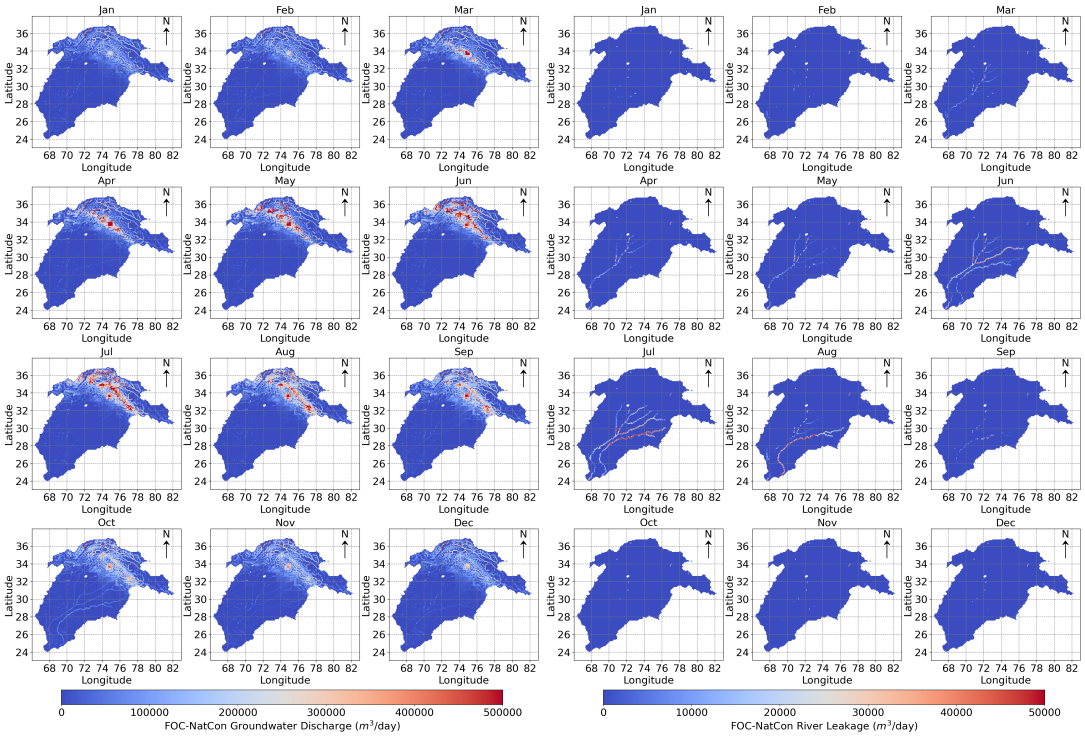

Figure 23 FOC-NatCon long-term monthly average groundwater discharge (left) and river leakage (right)

4.2 Human Impact Condition – HumanCon

Under OFC, the human impact condition model (OFC-HumanCon) was constructed and simulated to reflect the influence of human activities. Six cells from the three parts of the basin were selected to visualize the GWL variations during the period (Figure 10). Four of six show a GWL drawdown over the 30 years. Due to lower human activities in the upper basin and less water abstraction, the overall decline in water level in cells U1 and U2 is not significant, retaining a natural fluctuation pattern. Compared to this, there is a noticeable decline in GWL in the middle and lower basins from 1970 to 1999. Notably, areas near rivers exhibit relatively minor decreases in GWL, whereas significant declines are observed in the plains, especially in the middle basin where anthropogenic activities are more prevalent. Cell M1 experiences a drawdown of 5.99 m, while Cell L1 experiences a drawdown of 6.41 m in total (Figure 24). As the mid-lower basin experiences the most intense human activities, such a significant change in GWL is understandable and expected.

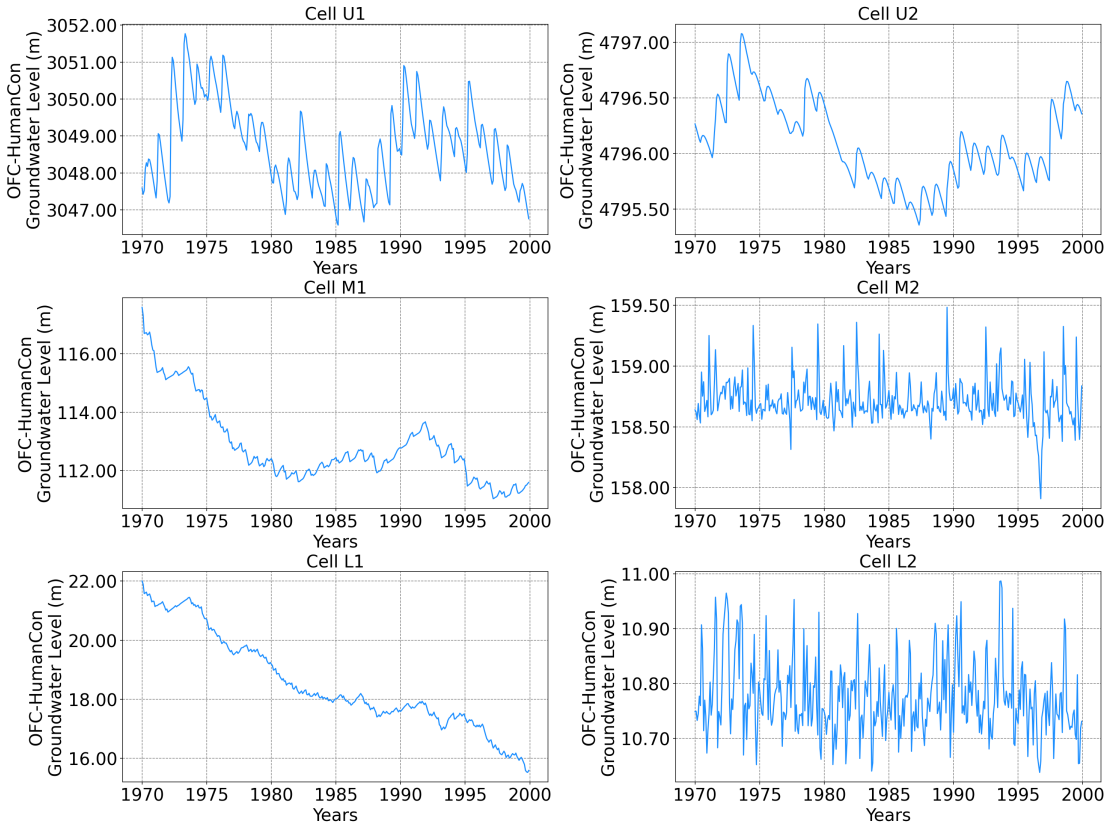

Figure 24 OFC-HumanCon six cells time-series plots of GWL

Under HumanCon, seasonal variations are influenced by anthropogenic groundwater abstraction from different sectors. In general, the GWL differences among twelve months at six cells range from 0.15 m to 1.47 m (Figure 25). In the upper basin, where abstraction activities are minimal, the seasonal GWL changes align with the recharge pattern (Figure 8). However, in the middle and lower basins, the four cells exhibit distinct seasonal behaviours, showcasing patterns entirely different from the recharge rate and natural GWL under NatCon. Although the overall interannual fluctuations are not significant, the peaks and troughs occur in different months, revealing spatial heterogeneity in the intensity of human activities. Meanwhile, this also suggests that anthropogenic groundwater abstraction activities occur consistently throughout the year, affecting GWL across the entire study area.

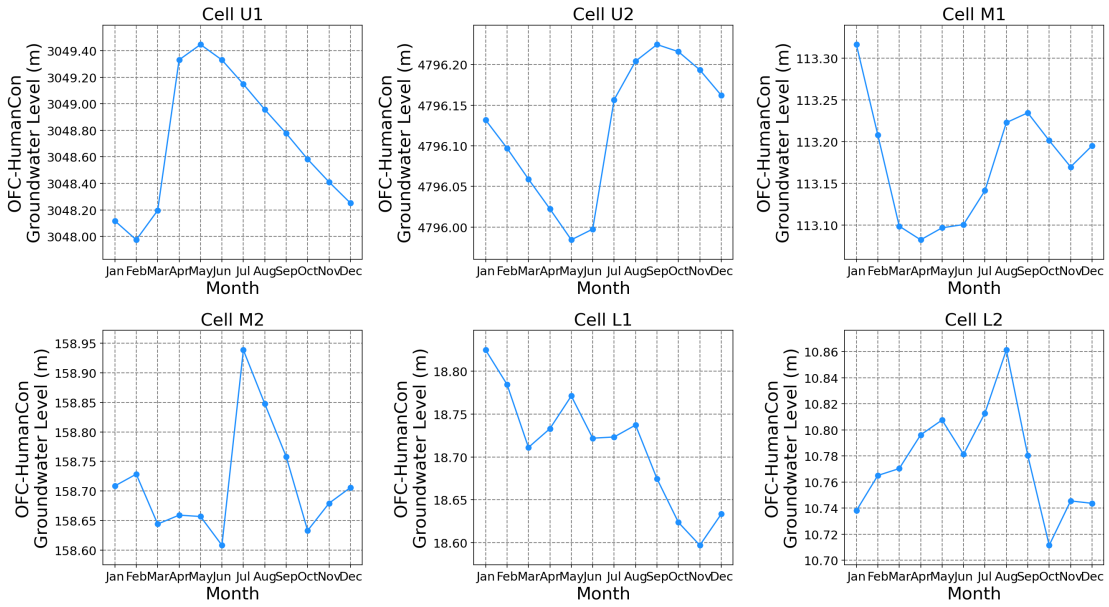

Figure 25 OFC-HumanCon six cells ltma of GWL

The GWL drawdown under HumanCon is much more significant than that under NatCon due to the intensive groundwater abstraction, with spatial variations. Here, there is no distinction made regarding the type of human activity. All sectors' water abstraction is calculated together. In total, about 15% of the basin don't have GWL decline, and 20% areas shows decline less than 10 m. Areas where the GWL declines by more than 50 m account for less than 0.5% of the entire basin. Zoom in on the sub-basins, in the upper basin, half of the areas never experience a decrease in GWL or even show increase, especially in the high mountainous area near the core of Himalayas. Most of the remaining areas here only have drawdowns of no more than 1 m (Figure 26). GWL decline primarily occurs in the middle and lower reaches, particularly in the plains of the middle basin and along the mainstream of the rivers. In the agriculture intensive area, over 80% of the region show GWL drawdown over 20 m within the 30 years, which illustrates the significant volume of human activity-related groundwater extraction. In lower basin, most areas near rivers experience GWL declines ranging from 1 to 10 m. In some isolated areas, drawdowns exceeding 20 m can occur.

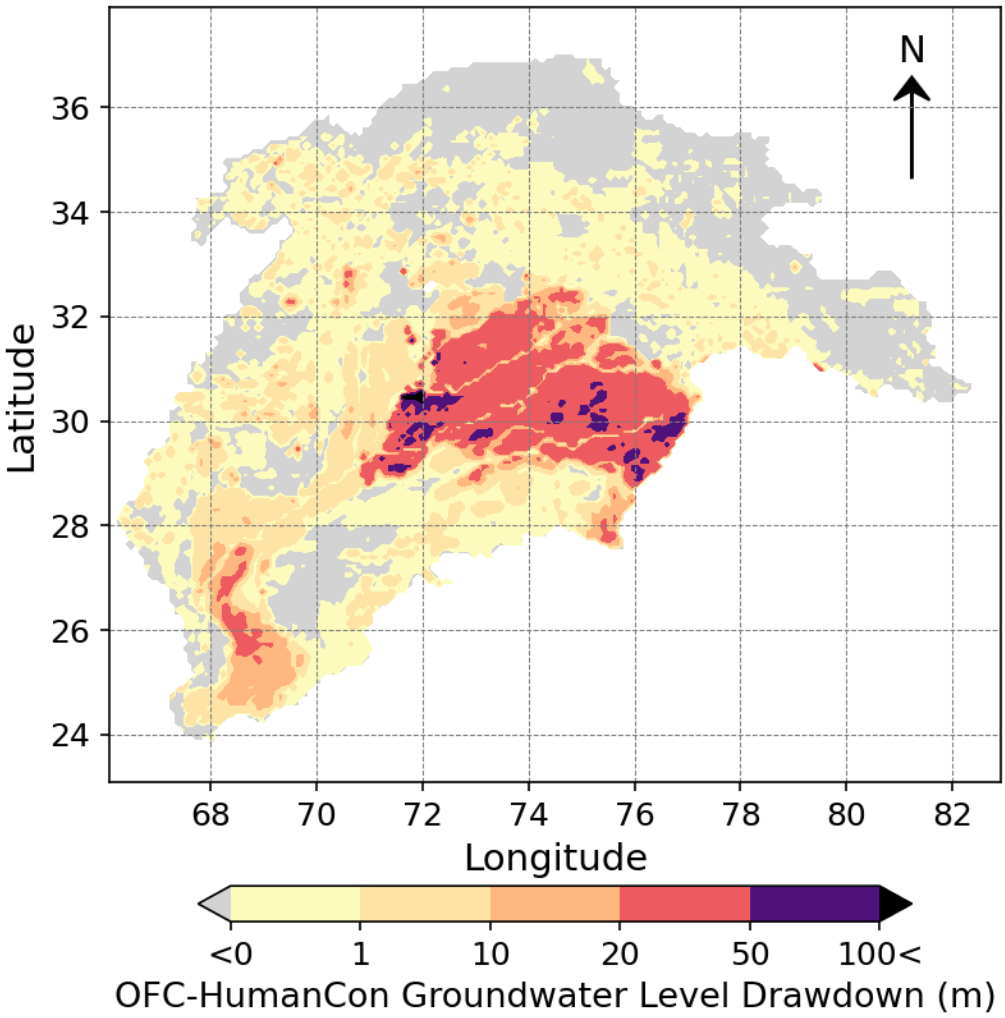

Figure 26 OFC-HumanCon groundwater level drawdown until 1999

Under HumanCon, as groundwater extraction from the aquifer continues, the baseflow exhibits a different pattern compared to NatCon (Figure 27). Within baseflow, both groundwater discharge and river leakage occur consistently throughout the year. In line with the NatCon, groundwater discharge persists at a notably higher level compared to river leakage. However, there has been a slight reduction in the disparity between the two. Under HumanCon, this ratio is 26.06. This indirectly indicates the impact of human activities on the groundwater system: more water loss from the top and reduced discharge to rivers. From the spatial perspective, in upper basin there is only groundwater discharge all the year and reaches its peak around summer-autumn. In middle and lower basin, river leaks to the aquifer almost the whole year. Only a small amount of groundwater discharge exists during the winter months.

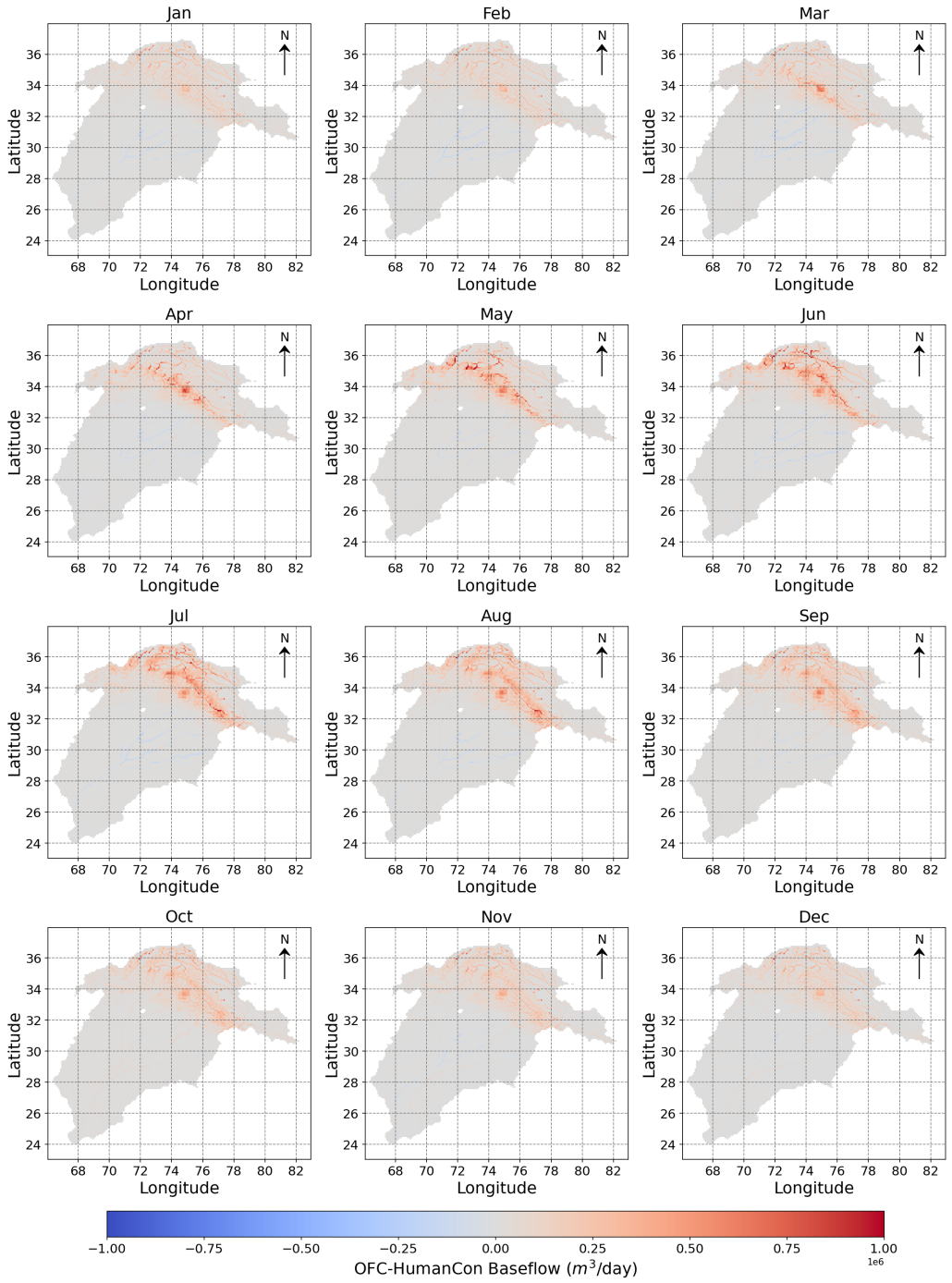

Figure 27 OFC-HumanCon long-term monthly average baseflow

Under HumanCon, the baseflow exhibits significant month-to-month variation, reflecting substantial long-term monthly average fluctuations. In upper basin it behaves similar to the NatCon. In the middle and lower basins, the long-term monthly average variation of baseflow lacks a discernible pattern. However, it can be seen that the GWL and baseflow still strongly influence each other (Figure 28). In general, the baseflow and GWL have a negative correlation. This is not changed by the anthropogenic water extraction. Remarkably, the baseflow values have undergone significant changes compared to NatCon. In Cells M3, M4, L3, and L4, the range of baseflow variation within twelve months is notably larger than that observed under NatCon.

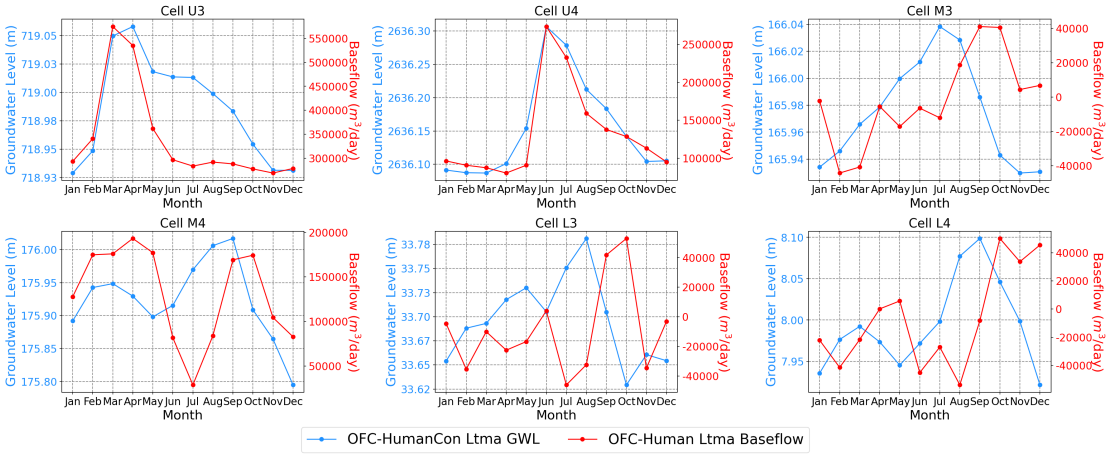

Figure 28 OFC-HumanCon long-term monthly average GWL and baseflow

4.3 Comparisons between NatCon and HumanCon

Comparing the simulated GWL under OFC-NatCon and OFC-HumanCon in December 1999, the GWL drawdown difference shows the impact of groundwater extractions by human on the groundwater system. Until 1999, the majority of the areas witnessed a decline in GWL ranging from 0 to 20 m. However, in the middle basin, certain areas exhibited drawdown exceeding 20 m. The annual average GWL drawdown was derived as 19 cm/yr in the whole basin. Droppers et al., (2022) derived the GWD in upper Indus Basin at a value of 9 cm/yr. (Cheema et al., (2014) calculated the GWD during the year 2007 at 12.1 cm. As the OFC model don't consider the baseflow interaction between the groundwater and river, it could lead to more severe of the GWL drawdown. In this model, compared with the NatCon, the six selected cells all show decline in GWL during the 30 years (Figure 29). As time progressed, the decline in GWL became more pronounced, particularly in the lower basin areas compared to the upper areas. In the upper basin, the decline in GWL was minimal, with only slight decreases observed in cells U1 and U2, registering 0.26 m and 0.01 m, respectively, until 1999. However, in the middle basin, the decline was more significant, with cell M1 experiencing an 8.15-m decrease and cell M2 showing a 0.20-m decrease. Similarly, cells L1 and L2 in the lower basin exhibited declines of 8.12 m and 0.12 m, respectively. The drawdown in M2 and L2 cells are similar. They are close to the river, so their GWL are affected by the river stage. Changes in river discharge also impact them, altering how they get replenished.

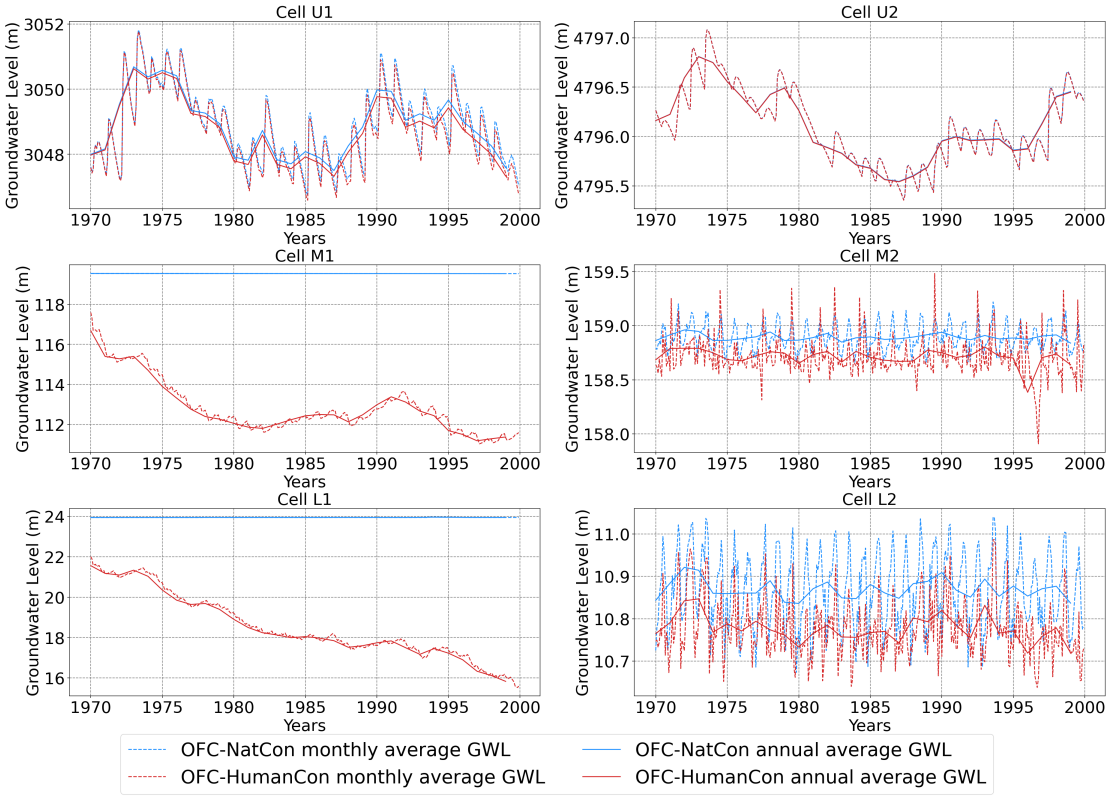

Figure 29 Comparisons between six cells OFC-NatCon and OFC-HumanCon

In general, the GWD proceeds at a steady pace, with more pronounced effects observed in the upper and middle basins compared to the lower basin. To provide a comprehensive understanding of GWD across different regions of the basin, three distinct frames were delineated: upper basin, middle basin, and lower basin, each exhibiting unique GWD behaviours (Figure 30). In the upper basin, GWD occurred at a very gradual rate, with some areas even experiencing an increase in groundwater storage during the initial decade, followed by minimal GWD thereafter. On average the number is 0.67 km^3/yr. Conversely, both the middle and lower basin areas consistently exhibited a decrease in groundwater storage throughout the simulation period. Of particular note is the agriculture-intensive region within the middle basin, where a substantial GWD was observed over the 30-year period. The average GWD in this area was calculated to be 56 km^3/yr, ranging from 0.1 km^3 to 5 km^3 per grid cell. In lower basin, the total GWD amounted to approximately 290 km^3 (on average 9.67 km^3/yr), with the majority concentrated near the river floodplain areas. Apparently, the estimated middle basin GWD in this model is greater than satellite-based calculation and sole groundwater model or hydrological model approach (Tiwari et al., 2009; Cheema et al., 2014; Droppers et al., 2020;). The absence of interaction with baseflow in the offline model likely accounts for the observed limitations. To address this issue and gain a more comprehensive understanding of the impact of human activities, future human impact models should be developed using online coupling schemes. By incorporating online coupling, which enables dynamic interactions between groundwater and surface water, these models can better capture the complexities of hydrological processes affected by human interventions which may provide more accurate assessments.

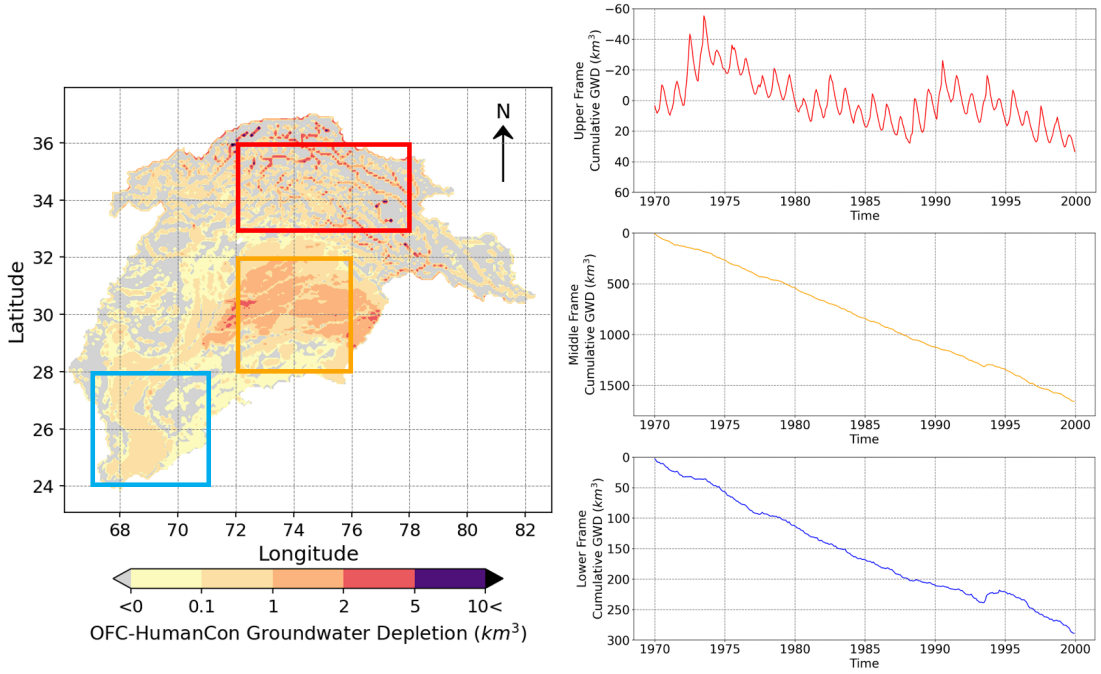

Figure 30 OFC-HumanCon GWD of different frames until 1999

Ch5 Discussions

5.1 Comparisons among three coupling schemes

By sequentially incorporating lateral and vertical interactions between groundwater and the surface water (including the vadose zone and rivers) into the model, the three coupling schemes show interesting result difference in terms of baseflow and GWL, highlighting the characteristics of using the coupling models.

The behaviour of baseflow in both offline and online coupling differs between positive and negative values, which is groundwater discharge and river leakage, respectively. In autumn and winter the groundwater discharge is more significant and, in spring and summer river leakage dominates in baseflow. Under OFC, there is no update between VIC-WUR and MODFLOW6 after each stress period. Under FOC, VIC-WUR accepts baseflow (negative or positive) from MODFLOW6 during each stress period. In this way, the water in river or groundwater can flow to recharge another, depends on the water level. As that the river stage is lower than GWL in some areas of the basin and within baseflow, the groundwater discharge is bigger than river leakage, by considering the interactions between surface water and groundwater, FOC simulates the long-term monthly average groundwater discharge higher than OFC at a mean ratio of 2.02% averaged over twelve months, mostly locate near the big rivers and mountainous area. The greatest difference occurs in February at a ratio of 6.58% while during summer and autumn the difference is within 1% (Figure 31 left). Moreover, nine out of twelve months show decrease in river leakage estimation under FOC, ranging from 17.49% in

August to 86.76% in February, locate only in and near river cells (Figure 31 right). These results match with the realistic interactions between surface river and groundwater. Compared to OFC, FOC takes baseflow into account in each stress period, which means the seasonal variation may influence the result. As river leakage almost all exist in mid-lower river streams, the calculated river stage under FOC became lower, resulted in more groundwater discharge and less river leakage here. Compared to the offline coupled scheme which lacks considering the interactions between surface water and groundwater, the coupling approach ensures a more physical representation in the hydrological system.

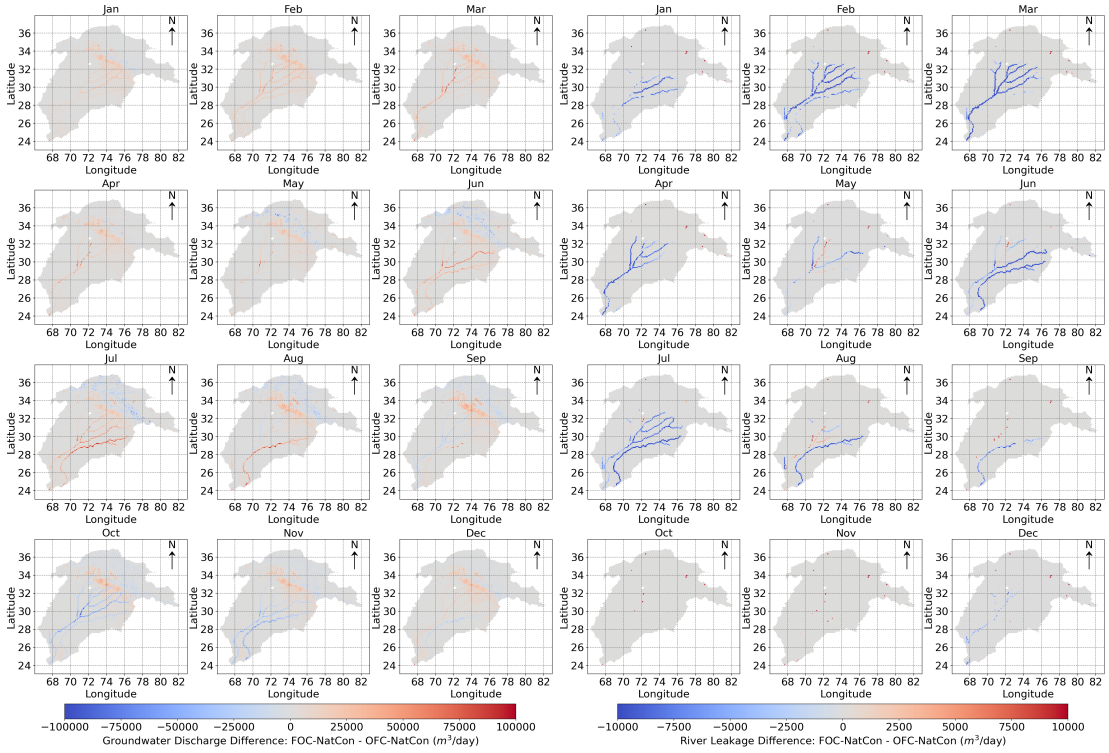

Figure 31 Groundwater discharge (left) and river leakage (right) difference between FOC-NatCon and OFC Nat-Con

Within all twelve months, compared to POC, FOC gives lower long-term monthly average groundwater discharge estimation, with a mean ratio of 0.29%. Almost all the differences occur in mid-upper basin mountainous area (Figure 32 left). For river leakage, in total FOC predicts 0.42% less than POC, concentrating in summer. In a spatial perspective, in upstream there is almost no difference in river leakage between two coupling schemes. Along with the river flows to downstream, it appears to exist (Figure 32 right). One explanation for this phenomenon lies in the topography of the northeast region of the Indus Basin, where the terrain is elevated, and the river stage remains relatively low. In such conditions, recharge from the river occurs only when the river stage substantially exceeds the GWL. While the differences in characteristics between FOC and POC may appear minor, when considering the baseflow volume, the variations between the results obtained from the two online coupling schemes can highlight the impact of capillary rise. It is essential to recognize that capillary rise

represents a significant component in hydrological models, and its contribution should not be overlooked.

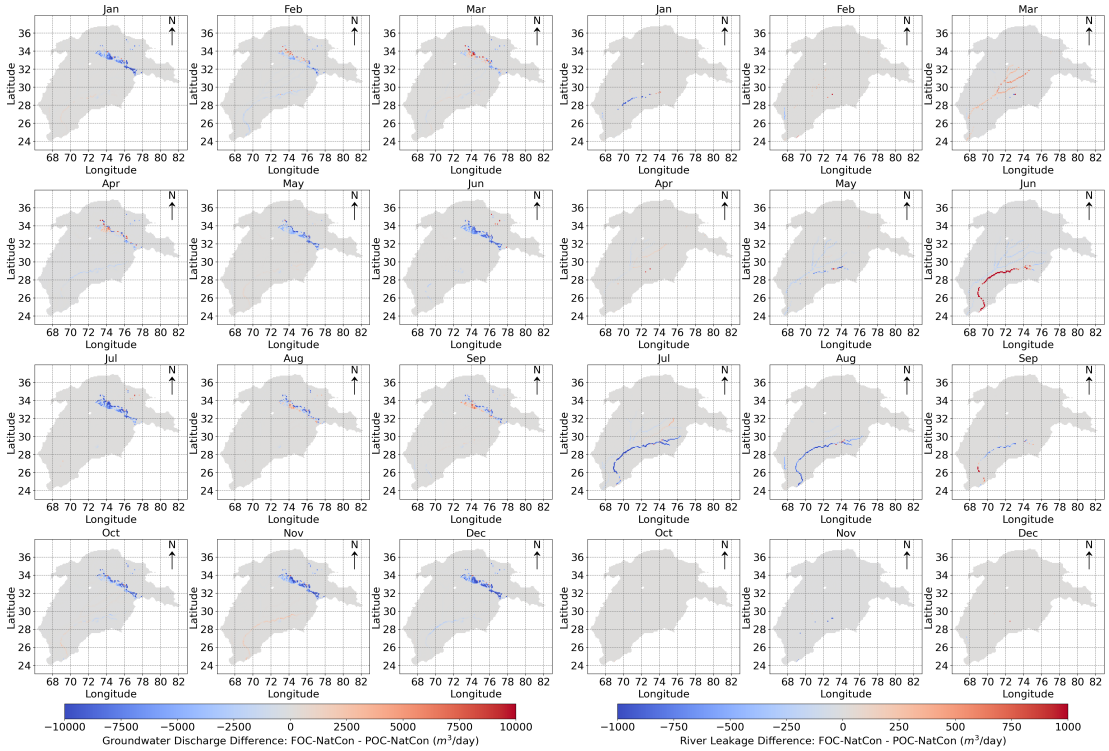

Figure 32 Groundwater discharge (left) and river leakage (right) difference between FOC-NatCon and POC Nat-Con

Compared to the two online coupling schemes, OFC exhibits more pronounced fluctuations in baseflow throughout the analysis period (Figure 33). This highlights the significant presence of subsurface flow dynamics in the Indus Basin. In the upper basin, where river discharge is low and terrain is elevated, the interactions between the river and groundwater are relatively minimal. Consequently, there are fewer differences in baseflow among the three modelling schemes, and the potential advantages of the coupling scheme are not fully realized. However, as water progresses downstream, the connectivity between groundwater and surface water becomes more pronounced, exerting a greater influence on the water system. Moreover, in the middle and lower basin, the simulated GWL under OFC are notably lower than those under POC and FOC (Figure 34). In MODFLOW6, this process is regulated by the RIV package. In offline coupling, the calculation of river stage relied solely on surface discharge, routed exclusively from surface runoff. However, in online coupling, the model accounted for the feedback of baseflow to the river, resulting in additional water being routed into or out of the model, depends on the spatial characteristics.

The difference between the two online coupling schemes is caused by the EVT package in MODFLOW6. When updating the capillary rise to VIC-WUR at the end of each stress period, a segment of groundwater in the vadose zone rises to the surface. This upward movement of water diminishes the volume of water directed to the river as baseflow, consequently contributing to a decline in the GWL. Furthermore, this process

can influence the groundwater baseflow and river leakage as it increases the variance between the river stage and the calculated GWL at the river cells.

In all, it reveals that in fact, the groundwater should be more affluent as during wet seasons it can decrease the discharge to river and river can also recharge to it in dry conditions, even though considering through capillary rise where groundwater loses water. In some areas, this kind of relationship may have the ability to increase the groundwater level, seen from cell M1 in Figure 33.

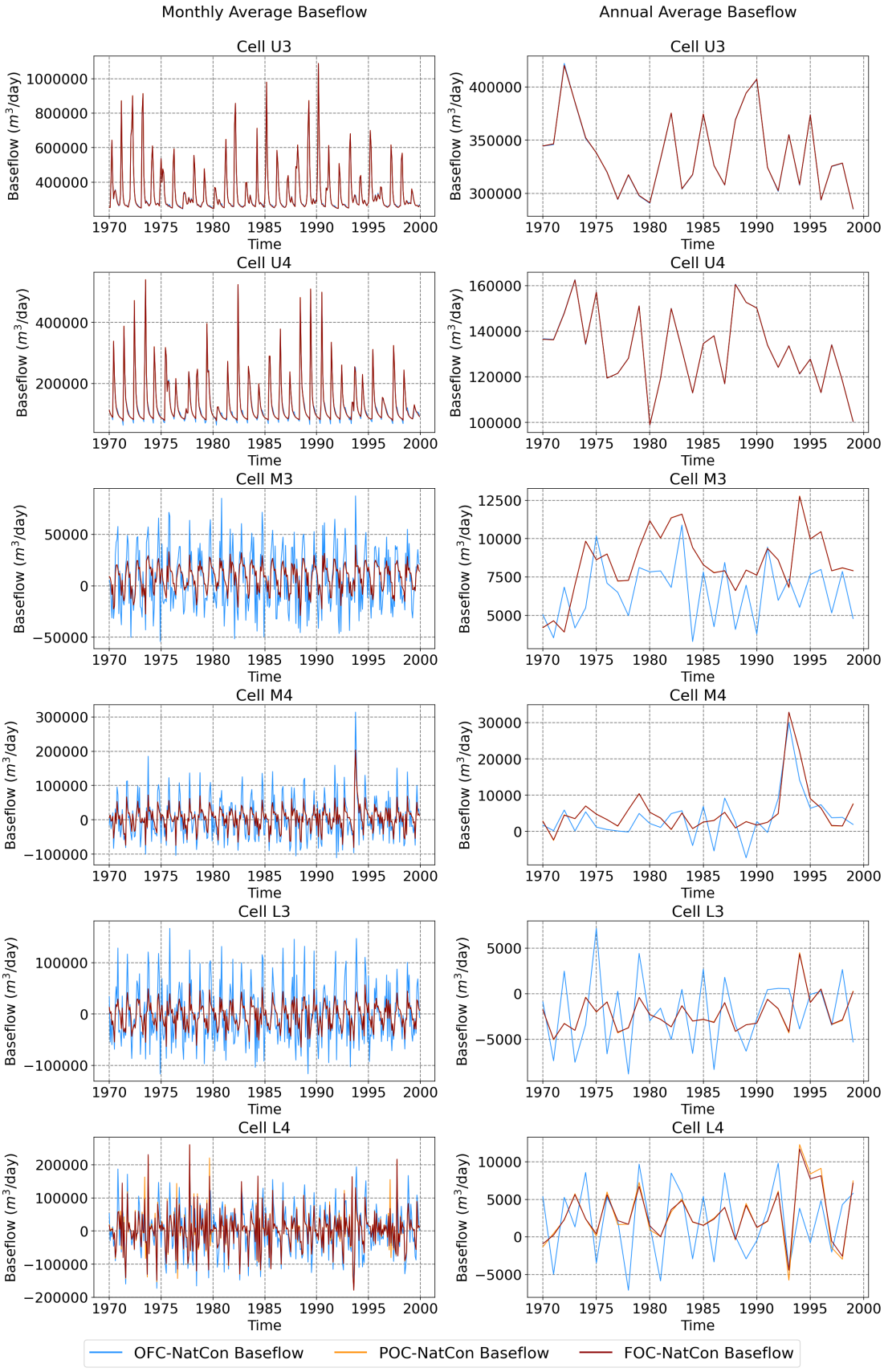

Figure 33 Monthly time-series baseflow of OFC, POC and FOC under NatCon

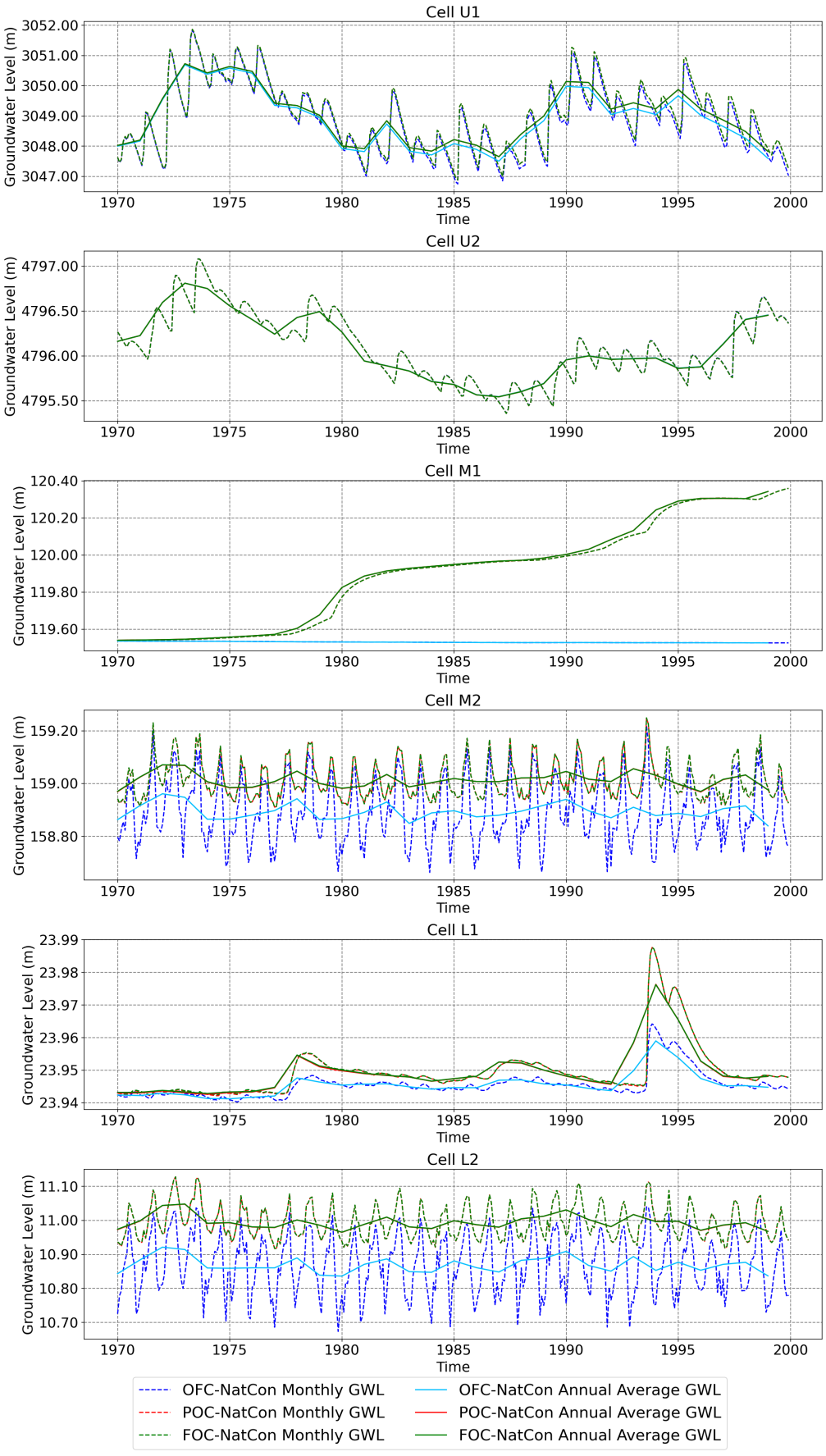

Figure 34 Monthly and annual time-series GWL under OFC-NatCon, POC-NatCon and FOC-NatCon

5.2 Comparisons between original VIC-WUR model and coupling models

This coupling scheme in Indus basin is tested by comparing the results of original VIC-WUR model with online coupling model (POC model and FOC model). In NatCon, by randomly selected another three river cells in each upstream, middle stream and downstream, it can be concluded that the coupling model VIC-WUR-MF predicts distinct river discharge differences compared to the original VIC-WUR model. In general, FOC model simulates the average river discharge lower than the original VIC-WUR model, due to the contribution of baseflow. The maximum discharge in the original VIC-WUR model is 12105.40 m^3/s while the number in FOC model is 11951.70 m^3/s. Meanwhile, there exists spatial variation. In the upstream, based on the three cells data, the FOC model simulates annual river discharge 7.00% lower than the original VIC-WUR model. While in the midstream and downstream, the coupling model simulates river discharge higher than the original VIC-WUR model with the value of about 4.97% and 0.23%, respectively. The variation in estimation arises from the model's coupling scheme design. Unlike reservoir-type representations used in the original VIC-WUR, the coupling model integrates real groundwater flow patterns. Consequently, this approach allows for a more accurate depiction of groundwater dynamics, resulting in a slightly higher overall water storage capacity in the groundwater system. The spatially heterogeneous distribution of baseflow and capillary rise across different sub-basins contributes to variations in the estimation of total river discharge. This emphasizes the importance of integrating both baseflow and capillary rise into hydrological models for more accurate predictions.

Moreover, the simulated average monthly discharge difference between the FOC model and the VIC-WUR model varies in a large range (Figure 35). The nine cells location can be found in Appendix C. During low-flow periods when the discharge is below the mean discharge, the FOC model yields mean river flow up to 2.53 times higher than the original VIC-WUR results. While during the period that the river is experiencing higher flows, the FOC model predicts up to 26.90% discharge lower than the original VIC-WUR model. It suggests that the existence of groundwater do influence the river runoff. During low flow periods, the groundwater acts as a buffer to stabilize river flows and, the river would leak to the groundwater when the river runoff goes too high in wet seasons. This difference could prove again that the interactions between groundwater and surface water do contribute a lot to the result of hydrological modelling. Taking this dynamic connection into consideration could enable the model to reveal more detailed variations of the surface water-groundwater system in Indus Basin.

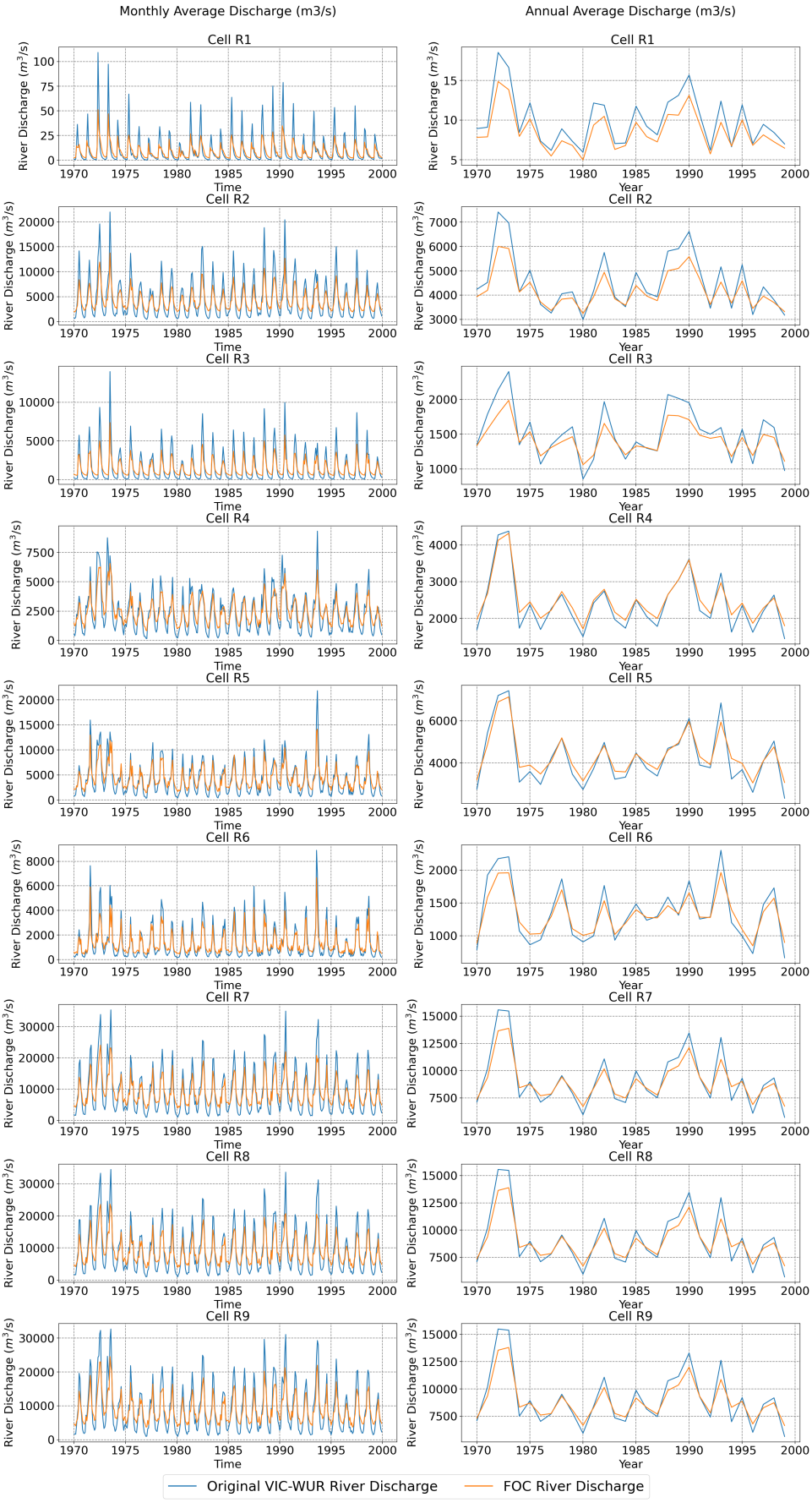

Figure 35 Nine cells monthly and annual average river discharge of original VIC-WUR and FOC

5.3 Uncertainty analysis

Due to the time limitation and some simplification in the methodology, this study still has several potential points worthy of discussion and improvement. In this study, the delineation between major rivers and smaller drains using 30 meters as a threshold for nodes is a detail worth further clarification. To determine the specific parameters of rivers in the Indus Basin and clarify the delineation between major rivers and smaller drains, as well as the flow characteristics of rivers in high mountainous regions, further investigation through more data collection and even field research is necessary. The current method of defining rivers may lead to inaccuracies in estimating baseflow, particularly in high mountainous areas where river water levels may be underestimated. The second point of improvement concerns the characterization of aquifer thickness. Due to data limitations, certain regions in this study lack specific information on aquifer thickness (missing value), and a uniform value of 200 m is assigned. Typically, aquifers in mountainous areas are thicker, and groundwater levels are deeper. Such simplifications may lead to insufficiently detailed characterization of groundwater flow and storage in mountainous regions. Furthermore, in this model, the initial conditions are set to steady-state conditions. It is believed that using the results of multiple spin-up iterations as initial conditions would better reflect real-world conditions. Finally, the excessive values of human activity extraction in this model may be attributed to the settings of VIC-WUR itself, as seen in Appendix D. Since this aspect is beyond the core scope of this study, it is suggested that if further development and optimization of VIC-WUR are considered in the future, attention should be paid to this issue.

5.4 Answers to research questions

Here the answers to the research questions in this study are summarized. In general, the impact of groundwater use on groundwater system with and without groundwater flow modelling have significant differences in terms of estimations of groundwater level, groundwater discharge, river leakage and total river runoff.

For research question 1: ‘What are the impacts of historical climate variations on groundwater flow system in Indus basin?’, the historical climate variations, in this study conceptualized as naturalized condition (NatCon), slightly influence the GWL by decreasing it within 1 m in 90% of the total basin. It simultaneously causes seasonal fluctuations in GWL, specifically, higher in summer and autumn, and lower in winter and spring. Upstream areas mainly generate groundwater discharge, which is 70 times greater than river leakage in the middle and downstream areas. Moreover, GWL and baseflow exhibit co-variation trends and show starkly contrasting trends in the middle and lower reaches. Also, when baseflow initiates a change, GWL exhibit a lagged response, consistently peaking up to a month later than baseflow.

For research question 2: ‘What are the impacts of human activities on groundwater flow system in Indus basin?’, in general, human beings affect groundwater flow system by extracting water in terms of various uses. The annual average GWL drawdown was

derived as 19 cm/yr in the whole basin. In total, about 15% of the basin does not have GWL decline. 20% areas show decline less than 10 m. Regions with GWL declines exceeding 50 meters comprise less than 0.5% of the basin. Regions adjacent to rivers demonstrate comparatively minimal reductions in GWL. However, substantial declines are evident in the mid-lower plains, particularly within the area where human activities exert a more pronounced influence. The total basin is also losing water storage during the 30 years. In upper basin, GWD occurs at a very gradual rate, 0.67 km^3/yr on average. with some areas even experiencing an increase at first. Both the middle and lower basin areas consistently exhibit a decrease in GWS. The middle agriculture-intensive region is observed 56 km^3/yr GWD over the 30-year period, ranging from 0.1 km^3 to 5 km^3 per grid cell in total. In lower basin, total GWD reaches around 290 km^3, mainly concentrated near river floodplains. The difference between groundwater discharge and river leakage diminishes, with a ratio of 26.

For research question 3: 'How does the groundwater impact the surface hydrological components in Indus Basin?', the groundwater does impact on the surface hydrological components in Indus Basin mainly through two ways: Produce capillary rise to the vadose zone and surface soil and interact with rivers by baseflow, which adjust the total river runoff. During low-flow periods, compared to without groundwater modelling, the groundwater flows to river up to 2.53 times higher. It acts as a buffer to stabilize river flows. While during high-flow periods, it forecasts up to 26.90% lower. The max discharge in the original VIC-WUR model is 12105.40 m^3/s while the number in FOC model is 11951.70 m^3/s. Meanwhile, in the upstream, the FOC model simulates annual river discharge 7.00% lower than the original VIC-WUR model. While in the midstream and downstream, FOC simulates river discharge higher than the original VIC-WUR model with the value of about 4.97% and 0.23%, respectively.

Ch6 Conclusions and Prospects

6.1 Conclusions

This study proposes a reliable surface water-groundwater coupling design, successfully tests it in the Indus Basin and discusses the weaknesses and strengths of different coupling schemes. During the process of the study, the following main conclusion statements can be drawn:

- The groundwater model in Indus Basin in naturalized condition is constructed and coupled with hydrological model built by VIC-WUR. The steady-state GWL ranges mainly from 0 to 6500 m during 1970 to 1999. In OFC, GWL fluctuates within 0.002 to 0.5 m, mostly with peak value around summer. The total groundwater discharge is approximately 70 times greater than river leakage. In POC and FOC, the groundwater discharge is primarily observed in the upper basin at a maximum of around 1.78 million m^3/day. The highest river leakage occurs in July at around 1100 m^3/day and lowest occurs in February at 37 m^3/day, with more variations in upper basin than lower basin.

- Human impacts are successfully simulated in OFC model. The six cells show GWL drawdown between 0.01 to 8.15 m. The annual average GWL drawdown was derived as 19 cm/yr in the whole basin. About 15% of the basin don't have GWL decline, and 20% areas show decline less than 10 meters. The hot spot area of GWD is in the middle agriculture intensive region and upper river streams. The GWD of three sub basins are 0.67 km^3/yr, 56 km^3/yr and 9.67 km^3/yr. The absence of interaction with baseflow in the offline model likely accounts for the high estimation of GWD compared to other studies. What's more, the difference between groundwater discharge and river leakage has a ratio of 26, lower than that under NatCon.

- The coupling models provide a more realistic estimation of the baseflow and prove that capillary rise is a non-neglectable sector in hydrological models. FOC simulates the groundwater discharge higher than the original VIC-WUR at a mean ratio of 2.02% for twelve months. Nine of twelve months show decrease in river leakage estimation under FOC, ranging from 17.49% in August to 86.76% in February. Moreover, compared to POC, FOC gives lower groundwater discharge estimation at a mean ratio of 0.29%. For river leakage, in total FOC predicts 0.42% less than POC, concentrating in summer.

- The interactions between groundwater and surface water do contribute a lot to the result of hydrological modelling. The maximum discharge in the original VIC-WUR model is 12105.40 m^3/s and the number in FOC model is 11951.70 m^3/s. In upstream, the FOC model simulates annual river discharge 7.00% lower than the original VIC-WUR model. In the midstream and downstream, the coupling model simulates river discharge higher than the original VIC-WUR model with the value

of 4.97% and 0.23%. During low-flow periods, the FOC model yields river flow mean value up to 2.53 times higher than the original VIC-WUR model. During high-flow period, the FOC model predicts up to 26.90% discharge lower than the original VIC-WUR model. Incorporating this dynamic connection could enhance the model's ability to capture detailed variations in the surface water-groundwater system in the Indus Basin.

6.2 Prospects

The successful development and application of the newly developed coupling model indicate the future potential to better estimate the hydrological process in surface water and groundwater and predict water availability. As the VIC-WUR model is really strong that it provides various vegetation types, is capable of simulating energy flux and can be coupled with other existing models such as MODFLOW and WOFOST, it could be believed that the coupled model developed in this study is worth to be applied and improved in the future. Without doubt, it does have room for improvement. If the dataset could be downscaled to a finer spatial resolution the accuracy can be strengthen. Moreover, the human impact condition in online coupling schemes is not applied in this study. If possible, the next step could be developing the fully coupling model under human impact condition, which can provide trusted prediction result in different future scenarios. What' more, currently the cost time of running the coupling model in one stress period is approximately 1 minute. If the model is going to extended to a global scale, it may cause some computational capability issues. If necessary, the I-O series of the model could be redesigned and improved to prevent repeating work in the simulation process. It will largely benefit to the total model performance.

References

Akhtar, F., Nawaz, R. A., Hafeez, M., Awan, U. K., Borgemeister, C., & Tischbein, B. (2022). Evaluation of GRACE derived groundwater storage changes in different agro-ecological zones of the Indus Basin. *Journal of Hydrology*, *605*. https://doi.org/10.1016/j.jhydrol.2021.127369

Ali, A. (2013). *Indus Basin Floods Mechanisms, Impacts, and Management*. Asian Development Bank. www.adb.org

Ali, S., Liu, D., Fu, Q., Cheema, M. J. M., Pal, S. C., Arshad, A., Pham, Q. B., & Zhang, L. (2022). Constructing high-resolution groundwater drought at spatio-temporal scale using GRACE satellite data based on machine learning in the Indus Basin. *Journal of Hydrology*, *612*. https://doi.org/10.1016/j.jhydrol.2022.128295

Arshad, A., Mirchi, A., Samimi, M., & Ahmad, B. (2022). Combining downscaled-GRACE data with SWAT to improve the estimation of groundwater storage and depletion variations in the Irrigated Indus Basin (IIB). *Science of the Total Environment*, *838*. https://doi.org/10.1016/j.scitotenv.2022.156044

Bonsor, H. C., MacDonald, A. M., Ahmed, K. M., Burgess, W. G., Basharat, M., Calow, R. C., Dixit, A., Foster, S. S. D., Gopal, K., Lapworth, D. J., Moench, M., Mukherjee, A., Rao, M. S., Shamsudduha, M., Smith, L., Taylor, R. G., Tucker, J., van Steenbergen, F., Yadav, S. K., & Zahid, A. (2017). Hydrogeological typologies of the Indo-Gangetic basin alluvial aquifer, South Asia. *Hydrogeology Journal*, *25*(5), 1377–1406. https://doi.org/10.1007/s10040-017-1550-z

Burek, P., Satoh, Y., Kahil, T., Tang, T., Greve, P., Smilovic, M., Guillaumot, L., Zhao, F., & Wada, Y. (2020). Development of the Community Water Model (CWatM v1.04) - A high-resolution hydrological model for global and regional assessment of integrated water resources management. *Geoscientific Model Development*, *13*(7), 3267–3298. https://doi.org/10.5194/gmd-13-3267-2020

Cheema, M. J. M., Immerzeel, W. W., & Bastiaanssen, W. G. M. (2014). Spatial quantification of groundwater abstraction in the irrigated indus basin. *Groundwater*, *52*(1), 25–36. https://doi.org/10.1111/gwat.12027

Cheema, M. J. M., & Qamar, M. U. (2019). Transboundary indus river basin: Potential threats to its integrity. In *Indus River Basin: Water Security and Sustainability* (pp. 183–201). Elsevier. https://doi.org/10.1016/B978-0-12-812782-7.00009-6

Condon, L. E., Kollet, S., Bierkens, M. F. P., Fogg, G. E., Maxwell, R. M., Hill, M. C., Fransen, H. J. H., Verhoef, A., Van Loon, A. F., Sulis, M., & Abesser, C. (2021). Global Groundwater Modeling and Monitoring: Opportunities and Challenges. In *Water Resources Research* (Vol. 57, Issue 12). John Wiley and Sons Inc. https://doi.org/10.1029/2020WR029500

Dahri, Z. H., Ludwig, F., Moors, E., Ahmad, B., Khan, A., & Kabat, P. (2016). An appraisal of precipitation distribution in the high-altitude catchments of the Indus basin. *Science of the Total Environment*, *548–549*, 289–306. https://doi.org/10.1016/j.scitotenv.2016.01.001

Dan, L., Ji, J., Xie, Z., Chen, F., Wen, G., & Richey, J. E. (2012). Hydrological

projections of climate change scenarios over the 3H region of China: A VIC model assessment. *Journal of Geophysical Research Atmospheres*, *117*(11). https://doi.org/10.1029/2011JD017131

de Graaf, I. E. M., Gleeson, T., (Rens) van Beek, L. P. H., Sutanudjaja, E. H., & Bierkens, M. F. P. (2019). Environmental flow limits to global groundwater pumping. *Nature*, *574*(7776), 90–94. https://doi.org/10.1038/s41586-019-1594-4

de Graaf, I. E. M., & Stahl, K. (2022). A model comparison assessing the importance of lateral groundwater flows at the global scale. *Environmental Research Letters*, *17*(4). https://doi.org/10.1088/1748-9326/ac50d2

de Graaf, I. E. M., van Beek, R. L. P. H., Gleeson, T., Moosdorf, N., Schmitz, O., Sutanudjaja, E. H., & Bierkens, M. F. P. (2017). A global-scale two-layer transient groundwater model: Development and application to groundwater depletion. *Advances in Water Resources*, *102*, 53–67. https://doi.org/10.1016/j.advwatres.2017.01.011

Döll, P., Fiedler, K., & Zhang, J. (2009). Global-scale analysis of river flow alterations due to water withdrawals and reservoirs. *Hydrol. Earth Syst. Sci*, *13*, 2413–2432. www.hydrol-earth-syst-sci.net/13/2413/2009/

Döll, P., Müller Schmied, H., Schuh, C., Portmann, F. T., & Eicker, A. (2014). Global-scale assessment of groundwater depletion and related groundwater abstractions: Combining hydrological modeling with information from well observations and GRACE satellites. *Water Resources Research*, *50*(7), 5698–5720. https://doi.org/10.1002/2014WR015595

Droppers, B., Franssen, W. H. P., Van Vliet, M. T. H., Nijssen, B., & Ludwig, F. (2020). Simulating human impacts on global water resources using VIC-5. *Geoscientific Model Development*, *13*(10), 5029–5052. https://doi.org/10.5194/gmd-13-5029-2020

Droppers, B., Supit, I., Leemans, R., van Vliet, M. T. H., & Ludwig, F. (2022). Limits to management adaptation for the Indus' irrigated agriculture. *Agricultural and Forest Meteorology*, *321*. https://doi.org/10.1016/j.agrformet.2022.108971

Gerdener, H., Kusche, J., Schulze, K., Döll, P., & Klos, A. (2023). The global land water storage data set release 2 (GLWS2.0) derived via assimilating GRACE and GRACE-FO data into a global hydrological model. *Journal of Geodesy*, *97*(7). https://doi.org/10.1007/s00190-023-01763-9

Gleeson, T., VanderSteen, J., Sophocleous, M. A., Taniguchi, M., Alley, W. M., Allen, D. M., & Zhou, Y. (2010). Groundwater sustainability strategies. In *Nature Geoscience* (Vol. 3, Issue 6, pp. 378–379). https://doi.org/10.1038/ngeo881

Gou, J., Miao, C., Duan, Q., Tang, Q., Di, Z., Liao, W., Wu, J., & Zhou, R. (2020). Sensitivity Analysis-Based Automatic Parameter Calibration of the VIC Model for Streamflow Simulations Over China. *Water Resources Research*, *56*(1). https://doi.org/10.1029/2019WR025968

Hamman, J. J., Nijssen, B., Bohn, T. J., Gergel, D. R., & Mao, Y. (2018). The variable infiltration capacity model version 5 (VIC-5): Infrastructure improvements for new applications and reproducibility. *Geoscientific Model Development*, *11*(8), 3481–3496. https://doi.org/10.5194/gmd-11-3481-2018

Hao, A., Zhang, Y., Zhang, E., Li, Z., Yu, J., Wang, H., Yang, J., & Wang, Y. (2018). Review: Groundwater resources and related environmental issues in China. *Hydrogeology Journal*, *26*(5), 1325–1337. https://doi.org/10.1007/s10040-018-1787-1

Harbaugh, A. W. (2005). *MODFLOW-2005, The U.S. Geological Survey Modular Ground-Water Model-the Ground-Water Flow Process (Vol. 6)*. http://water.usgs.gov/software/ground_water.html/.

Janjua, S., Hassan, I., Muhammad, S., Ahmed, S., & Ahmed, A. (2021). Water management in Pakistan's Indus Basin: challenges and opportunities. *Water Policy*, *23*(6), 1329–1343. https://doi.org/10.2166/wp.2021.068

Khadri, S. F. R., & Pande, C. (2016). Ground water flow modeling for calibrating steady state using MODFLOW software: a case study of Mahesh River basin, India. *Modeling Earth Systems and Environment*, *2*(1). https://doi.org/10.1007/s40808-015-0049-7

Khan, A. J., Koch, M., & Tahir, A. A. (2020). Impacts of climate change on thewater availability, seasonality and extremes in the Upper Indus Basin (UIB). *Sustainability (Switzerland)*, *12*(4). https://doi.org/10.3390/su12041283

Konikow, L. F. (2011). Contribution of global groundwater depletion since 1900 to sea-level rise. *Geophysical Research Letters*, *38*(17). https://doi.org/10.1029/2011GL048604

Kuang, X., Liu, J., Scanlon, B. R., Jiao, J. J., Jasechko, S., Lancia, M., Biskaborn, B. K., Wada, Y., Li, H., Zeng, Z., Guo, Z., Yao, Y., Gleeson, T., Nicot, J.-P., Luo, X., Zou, Y., & Zheng, C. (2024). The changing nature of groundwater in the global water cycle. *Science*, *383*(6686). https://doi.org/10.1126/science.adf0630

Laghari, A. N., Vanham, D., & Rauch, W. (2012). The Indus basin in the framework of current and future water resources management. *Hydrology and Earth System Sciences*, *16*(4), 1063–1083. https://doi.org/10.5194/hess-16-1063-2012

Langevin, C. D., Hughes, J. D., Banta, E. R., Niswonger, R. G., Panday, S., & Provost, A. M. (2017). *Documentation for the MODFLOW 6 Groundwater Flow Model: U.S. Geological Survey Techniques and Methods, book 6, chap. A55*.

Liang, X., Lettenmaier, D. P., Wood, E. F., & Burges, S. J. (1994). A simple hydrologically based model of land surface water and energy fluxes for general circulation models. *Journal of Geophysical Research*, *99*(D7). https://doi.org/10.1029/94jd00483

Lohmann, D., Nolte-Holube, R., & Raschke, E. (1996). A large-scale horizontal routing model to be coupled to land surface parametrization schemes. *Tellus, Series A: Dynamic Meteorology and Oceanography*, *48*(5), 708–721. https://doi.org/10.3402/tellusa.v48i5.12200

Mcdonald, M. G., & Harbaugh, A. W. (1984). *A modular three-dimensional finite-difference ground-water flow model*.

Qureshi, A. S., McCornick, P. G., Sarwar, A., & Sharma, B. R. (2010). Challenges and Prospects of Sustainable Groundwater Management in the Indus Basin, Pakistan. *Water Resources Management*, *24*(8), 1551–1569. https://doi.org/10.1007/s11269-009-9513-3

Shamsudduha, M., Taylor, R. G., Ahmed, K. M., & Zahid, A. (2011). The impact of intensive groundwater abstraction on recharge to a shallow regional aquifer system: Evidence from Bangladesh. *Hydrogeology Journal*, *19*(4), 901–916. https://doi.org/10.1007/s10040-011-0723-4

Shrestha, A., Agrawal, N., Alfthan, B., Bajracharya, S., Maréchal, J., & van Oort, B. eds. (2015). *The Himalayan Climate and Water Atlas; Impact of Climate Change on Water Resources in Five of Asia's Major River Basins*.

Shrestha, A. B., Wagle, N., & Rajbhandari, R. (2019). A review on the projected changes in climate over the indus basin. In *Indus River Basin: Water Security and Sustainability* (pp. 145–158). Elsevier. https://doi.org/10.1016/B978-0-12-812782-7.00007-2

Smolenaars, W. J., Dhaubanjar, S., Jamil, M. K., Lutz, A., Immerzeel, W., Ludwig, F., & Biemans, H. (2022). Future upstream water consumption and its impact on downstream water availability in the transboundary Indus Basin. *Hydrology and Earth System Sciences*, *26*(4), 861–883. https://doi.org/10.5194/hess-26-861-2022

Sood, A., & Smakhtin, V. (2015). Global hydrological models: a review. *Hydrological Sciences Journal*, *60*(4), 549–565. https://doi.org/10.1080/02626667.2014.950580

Tiwari, V. M., Wahr, J., & Swenson, S. (2009). Dwindling groundwater resources in northern India, from satellite gravity observations. *Geophysical Research Letters*, *36*(18). https://doi.org/10.1029/2009GL039401

Vinca, A., Parkinson, S., Riahi, K., Byers, E., Siddiqi, A., Muhammad, A., Ilyas, A., Yogeswaran, N., Willaarts, B., Magnuszewski, P., Awais, M., Rowe, A., & Djilali, N. (2021). Transboundary cooperation a potential route to sustainable development in the Indus basin. *Nature Sustainability*, *4*(4), 331–339. https://doi.org/10.1038/s41893-020-00654-7

Wada, Y., Van Beek, L. P. H., Van Kempen, C. M., Reckman, J. W. T. M., Vasak, S., & Bierkens, M. F. P. (2010). Global depletion of groundwater resources. *Geophysical Research Letters*, *37*(20). https://doi.org/10.1029/2010GL044571

Wang, G. Q., Zhang, J. Y., Jin, J. L., Pagano, T. C., Calow, R., Bao, Z. X., Liu, C. S., Liu, Y. L., & Yan, X. L. (2012). Assessing water resources in China using PRECIS projections and a VIC model. *Hydrology and Earth System Sciences*, *16*(1), 231–240. https://doi.org/10.5194/hess-16-231-2012

Wang, S., Shao, J., Song, X., Zhang, Y., Huo, Z., & Zhou, X. (2008). Application of MODFLOW and geographic information system to groundwater flow simulation in North China Plain, China. *Environmental Geology*, *55*(7), 1449–1462. https://doi.org/10.1007/s00254-007-1095-x

Winter, T. C., Harvey, J. W. (Judson W., Franke, O. L., Alley, W. M., & Geological Survey (U.S.). (1998). *Ground water and surface water : a single resource*. U.S. Geological Survey.

Xu, X., Huang, G., Zhan, H., Qu, Z., & Huang, Q. (2012). Integration of SWAP and MODFLOW-2000 for modeling groundwater dynamics in shallow water table areas. *Journal of Hydrology*, *412–413*, 170–181. https://doi.org/10.1016/j.jhydrol.2011.07.002

Yu, L., Ding, Y., Chen, F., Hou, J., Liu, G., Tang, S., Ling, M., Liu, Y., Yan, Y., & An, N. (2018). Groundwater resources protection and management in China. *Water Policy*, *20*(3), 447–460. https://doi.org/10.2166/wp.2017.035

Appendix

Appendix A: idomin setting

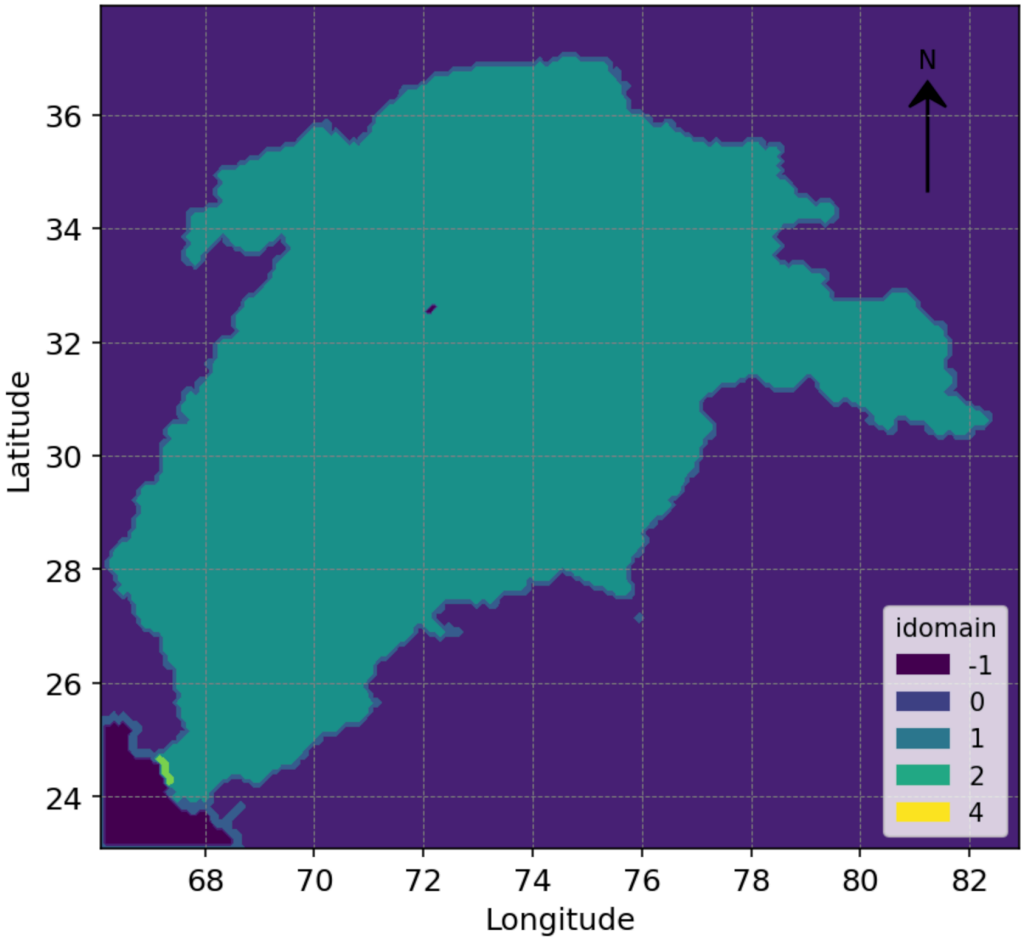

Appendix B: Full input lists

Dataset	Use
Clone_05min.nc	To do geological transformation
demfrom30s.nc	Indus Basin terrain
damc_ave.nc	Initial aquifer depth
lkmc_ave.nc	To define hydraulic conductivity
Indus_CellArea_m2_05min.nc	Area of each grid cell
Qbank_new_average.nc	To calculate river width
slope05min_avgFrom30sec.nc	The slope of the river channel
efplact_new_05min.nc	Floodplain level
mindem_05min.nc	DEM used to define river head
conflayers4.nc	Separate confine and unconfine layers
kl1B_ave.nc	To define top layer hydraulic conductivity
kl2B_ave.nc	To define bottom layer hydraulic conductivity
StorCoeff_NEW.nc	Specific yield
boundary.nc	To define the boundary
topl1_gwl_Indus_monthly_1968to2000.nc	Top layer groundwater constant head
topl2_gwl_Indus_monthly_1968to2000.nc	Bottom layer groundwater constant head
Indus_gwl_steady_state_final.nc	Steady-state groundwater level
VIC_params_Modis_calibrated_Indus.nc	VIC-WUR parameters
CPsurface.nc	Information of elevation, flux rate and extinction depth of capillary rise

Appendix C: Location of nine selected cells in discussion

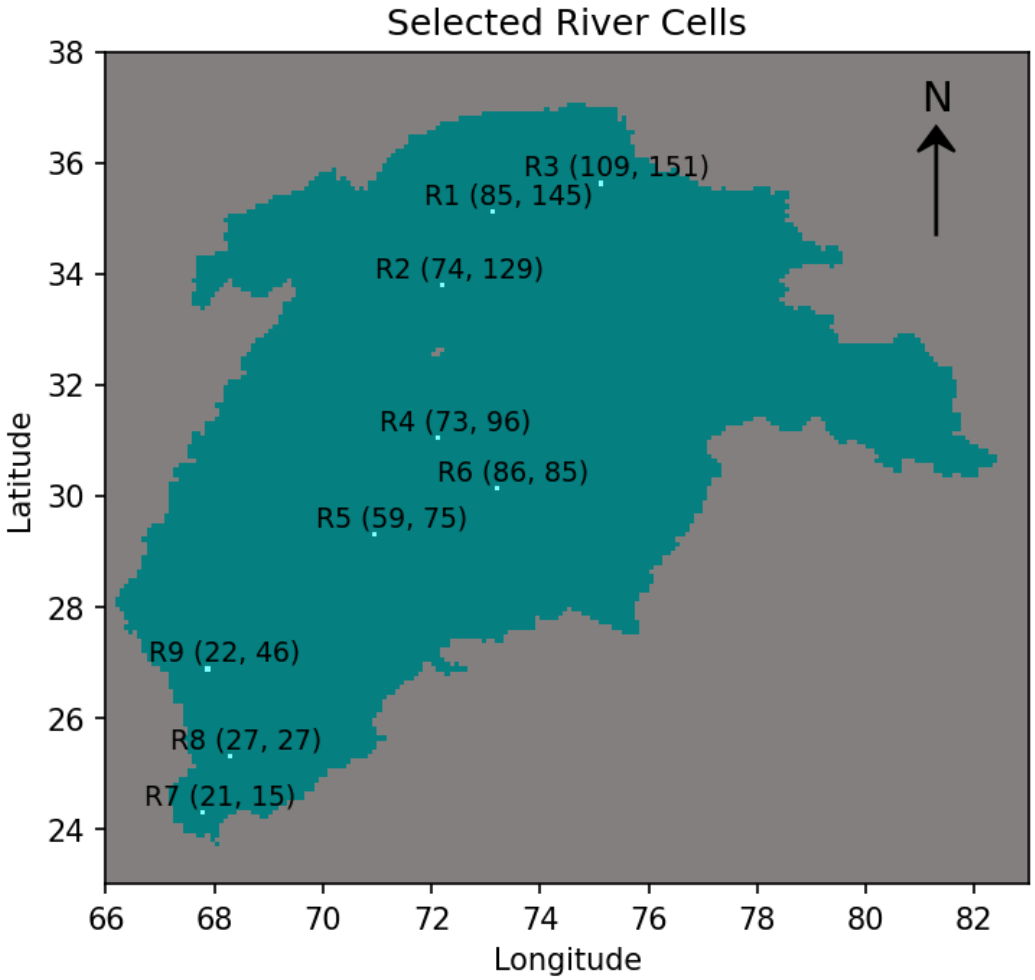

Appendix D: Average human impact groundwater extraction